CEA-R-6227

ISSN 0429 - 3460

COMMISSARIAT À L'ÉNERGIE ATOMIQUE

DIRECTION DE L'ÉNERGIE NUCLÉAIRE

UNRESOLVED RESONANCE RANGE CROSS SECTION PROBALITY AND SELF SHIELDING FACTORS

par

Jean-Christophe SUBLET*

Roger N. BLOMQUIST (Argonne National Laboratory,USA)

Sedat GOLUOGLU (Oak Ridge National Laboratory, USA)

Robert E. MAC FARLANE (Los Alamos National Laboratory, USA)

CEA CADARACHE

*DIRECTION DE L'ÉNERGIE NUCLÉAIRE

DÉPARTEMENT D'ÉTUDES DES RÉACTEURS

SERVICE DE PHYSIQUE DES RÉACTEURS ET DU CYCLE

LABORATOIRE D'ÉTUDES DE PHYSIQUE

DIRECTION DES SYSTÈMES D'INFORMATION

CEA / SACLAY 91191 GIF-SUR-YVETTE CEDEX FRANCE

2009

RAPPORT

CEA-R-6227

Rapport CEA-R-6227 -

CEA Cadarache
*Direction de L'Énergie Nucléaire
Département d'Études des Réacteurs
Service de Physique des Réacteurs et du Cycle
Laboratoire d'Études de Physique

UNRESOLVED RESONANCE RANGE CROSS SECTION PROBALITY AND SELF SHIELDING FACTORS

by

Jean-Christophe Sublet *
Roger N. Blomquist
(Argonne National Laboratory, USA)
Sedat Goluoglu
(Oak Ridge National Laboratory, USA)
Robert E. MacFarlane
(Los Alamos National Laboratory, USA)

- Juillet 2009 -

RAPPORT CEA-R-6227 – Jean-Christophe Sublet, Roger N. Blomquist, Sedat Goluoglu, Robert E. MacFarlane

«Sections Efficaces dans le Domaine non-résolu, Tables de Probabilités et Facteurs d'Auto Protection»

Résumé **-** Les méthodes et performances de quatre codes de traitements sont comparées dans le domaine non-résolu d'une sélection d'évaluations. Les évaluations ont été choisies de manière à faire un bilan de ce que contiennent les bibliothèques majeures telles que, ENDF/B-VII ou JEFF-3.1.1. Les résultats comparatifs sont accompagnés d'études détaillées concernant les formats et formalismes utilisés ainsi que leur interprétation au travers des codes de traitements.
Après quelques itérations, les résultats montrent un assez bon accord en ce qui concerne les sections efficaces à dilution infinie. De bien plus large différences apparaissent quand les sections effectives auto-protégées sont comparées. Les sections à dilution infinie sont souvent bien graphiquement connues, cependant ce sont les sections effective auto protégées dérivées des tables de probabilités qui sont réellement utilisées et interprétées par les codes de transport et de criticité dans ce domaine en énergie. Cette étude suggère que les formats et formalismes utilisés dans le domaine énergétique non-résolu des évaluations existantes soient révisés et toutes ambiguïtés levées. Il serait aussi souhaitable que le calcul des sections effectives auto-protégées par les différents codes converge avec une précision accrue.

2009 – Commissariat à l'Énergie Atomique – France

RAPPORT CEA-R-6227 – Jean-Christophe Sublet, Roger N. Blomquist, Sedat Goluoglu, Robert E. MacFarlane

«Unresolved Resonance Range Cross Section, Probability Tables and Self Shielding Factors»

Abstract **-** The performance and methodology of four processing codes have been compared in the unresolved resonance range of a selected set of isotopes. Those isotopes have been chosen to encompass most cases encountered in the unresolved energy range contained in major libraries like ENDF/B-VII or JEFF-3.1.1. The code results comparison is accompanied by data format and formalism examinations and processing code fine-interpretation study.
After some improvements, the results showed generally good agreement, although not perfect with infinitely dilute cross sections. However, much larger differences occur when shelf-shielded effective cross sections are compared. The infinitely dilute cross section are often plot checked but it is the probability table derived and self-shielded cross sections that are used and interpreted in criticality and transport calculations. This suggests that the current evaluation data format and formalism, in the unresolved resonance range should be tightened up, ambiguities removed. In addition production of the self shielded cross sections should be converged to a much greater accuracy.

2009 – Commissariat à l'Énergie Atomique – France

ISSN 0429 - 3460

Rapport CEA-R-6227-

Unresolved Resonance Range Cross Section, Probability Tables and Self Shielding Factors

by

Jean-Christophe Sublet (CEA, DEN, Cadarache, France)
Roger N. Blomquist (Argonne National Laboratory, USA)
Sedat Goluoglu (Oak Ridge National Laboratory, USA)
Robert E. MacFarlane (Los Alamos National Laboratory, USA)

June 11, 2009

Abstract

The performance and methodology of four processing codes have been compared in the unresolved resonance range of a selected set of isotopes. Those isotopes have been chosen to encompass most cases encountered in the unresolved energy range contained in major libraries like ENDF/B-VII or JEFF-3.1.1. The code results comparison is accompanied by data format and formalism examinations and processing code fine-interpretation study.

After some improvements, the results showed generally good agreement, although not perfect with infinitely dilute cross sections. However, much larger differences occur when shelf-shielded effective cross sections are compared. The infinitely dilute cross section are often plot checked but it is the probability table derived and self-shielded cross sections that are used and interpreted in criticality and transport calculations. This suggests that the current evaluation data format and formalism, in the unresolved resonance range should be tightened up, ambiguities removed. In addition production of the self shielded cross sections should be converged to a much greater accuracy.

Sections Efficaces dans le Domaine Non-Résolu, Tables de Probabilités et Facteurs d'Auto Protection

Résumé

Les méthodes et performances de quatre codes de traitements sont comparées dans le domaine non-résolu d'une sélection d'évaluations. Les évaluations ont été choisies de manière à faire un bilan de ce que contiennent les bibliothèques majeures telles que, ENDF/B-VII ou JEFF-3.1.1. Les résultats comparatifs sont accompagnés d'études détaillées concernant les formats et formalismes utilisés ainsi que leur interprétation au travers des codes de traitements.

Après quelques itérations, les résultats montrent un assez bon accord en ce qui concerne les sections efficaces à dilution infinie. De bien plus large différences apparaissent quand les sections effectives auto-protégées sont comparées. Les sections à dilution infinie sont souvent bien graphiquement connues, cependant ce sont les sections effective auto protégées dérivées des tables de probabilités qui sont réellement utilisées et interprétées par les codes de transport et de criticité dans ce domaine en énergie. Cette étude suggère que les formats et formalismes utilisés dans le domaine énergétique non-résolu des évaluations existantes soient révisés et toutes ambiguïtés levées. Il serait aussi souhaitable que le calcul des sections effectives auto-protégées par les différents codes converge avec une précision accrue.

Disclaimer

Neither the authors nor CEA, ANL, ORNL or LANL accepts responsibility for consequences arising from any errors either in the present documentation or in the cross section libraries and tables therein described.

Acknowledgements

The authors would like to acknowledge the instrumental and constructive contributions of D. E. Cullen (Lawrence Livermore National Laboratory) and C. R. Lubitz (Knolls Atomic Power Laboratory). One author (JCS) wishes to acknowledge the contributions of P. Ribon (CALENDF's real father)

Corresponding author: jean-christophe.sublet@cea.fr

Tables of contents

1 Introduction

There have been significant improvements in our capabilities to predict nuclear criticality and shielding experiments in recent years. This has been due to many factors, one of them being improved nuclear data evaluations properly handled by our processing codes. This allows to begun paying more attention to what always has been thought to be an important energy range, but not too well comprehended: the unresolved energy range [1]. It is clear that this intermediate energy range play a prominent role in many applications, not only the so called fast ones. The tendency of neutrons to slow down from a mean fission energy indicates that it is only a passing, transitory range for the thermal driven plant but quickly becomes an important integral response range for plants sensitive to the unresolved variety of its main constituent isotopes. It is clear as well that cladding, shielding, coating or many structural materials also have an unresolved resonance range that need to be accounted for.

This report is intended to be a contribution to the form of representation of unresolved resonance regions in the ENDF-102 data format [2], and the interpretation of the format by processing codes. Evaluator and engineer tend to plot the cross sections versus energy mostly infinitely dilute and rarely the self shielded form of the data. All comparisons are usually made at that infinite dilute level although criticality or transport codes rarely use this level of representation having to account for dilution effects. Validation, qualifications and benchmarking exercises also rely on shielded processed data to compute their results, although their feedback and interpretation are usually weighted and applied on the infinitely dilute level.

It is for all these reasons that we reassessed our interpretation capabilities in the unresolved energy range, highlighting their effects on the cross sections that shape the neutron transport and criticality code computational results.

2 Unresolved resonance range computation

In the unresolved region the cross sections are computed from file 2 (resonance parameters) and file 3 (cross sections) following the rules set in the ENDF-102 Data formats and procedures for ENDF data file report [2]. It stipulates that in this energy range only Single Level Breit-Wigner SLBW formalism is allowed. However several options are available for specifying the energy dependence of the parameters. Let us only consider the energy-dependent UR format (LRF=2). It provides average resonance parameters on a grid of energies and an interpolation code INT. The current ENDF procedures say that one should compute the unresolved cross sections at these energy grid points. Intermediate values are to be obtained by interpolating on the cross sections using the scheme defined by INT. This approach has the advantage of being economical in the UR calculation and of giving a unique result for the cross sections. However, the cross sections that it produces have discrete segments that show up as straight unphysical lines when plotted according to INT.

The PREPRO processing code [3] computes new parameters at intermediate energies using the interpolation law INT, and then it uses these new parameters to compute the cross sections at the intermediate points. It continues subdividing intervals until it ends up with linearly interpolated cross sections on a finer grid that are within a specified tolerance of the shape that comes from the UR formulas. This deviation from the rules stems from the fact that another recommendation made in the ENDF-102 manual is largely ignored by the

evaluators. They also should supply parameters on a dense enough grid to insure no significant difference (percent levels) between parameter or cross section interpolation. In interpolating the parameters to a finer grid the processing code compensates for crude and non ENDF-102 compliant unresolved resonance range parameters sets. Those findings have led to a modifications proposal [4] made in 2009 to the ENDF-102 governing board.

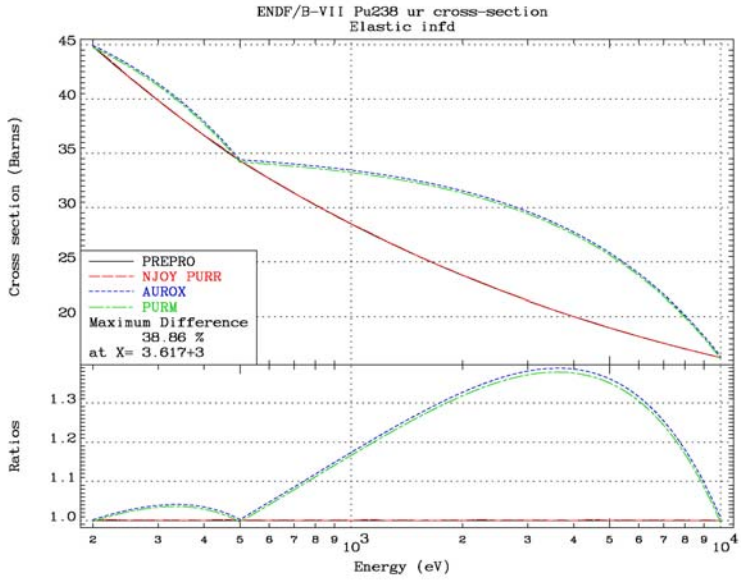

Figure 1 UR cross sections comparisons – 4 codes

The NJOY [5] results quoted in this study embed this new recommendation, in contrast to earlier pre NJOY-259 versions (giving results similar to AUROX), having been computed with the -296 version of the code, while it can be seen from Fig. 1 that neither AUROX [6] nor PURM [7] did it yet, nothing in principal would stop them to do so in the near future.

It should be clear also that the CALENDF [8] method and philosophy are more in line with the PREPRO ones, although this particular code takes rather different approaches.

To weigh the effects of the UR parameters interpretations, it is useful to examine the existing ENDF/B-VII [9] evaluations to see how they are affected by those issues and to see how serious interpretation problem might be in practice. The factors that influence this include how many energy grid points were used, what the step size is between two energies, what value was used for INT, and how smoothly the parameters vary with energy.

Evaluations with smoothly varying parameters were developed based on theory and systematics with a minimum of adjustment to experiment. They make up the large majority of the ENDF/B-VII evaluations. In the selected set of evaluations of Tables I, these will be labeled with a shape of constant or lin-lin. In a few cases, parameters were adjusted to fit high resolution experimental data. Those parameters normally fluctuate strongly and don't show a smooth variation with energy. They are labeled as "rough" in the tables. Another complication comes from competitive reactions like inelastic scattering. Then the competitive Γ_x width can vary strongly even though the other parameters are smooth. The ENDF-102 LSSF flag indicates, when equal to 1, that the file 2 parameters are to be used uniquely for shelf-shielding the cross section that are normalized to the values contained in file 3.

Computation of the effective cross section in the unresolved range may be done in different ways. The first is direct calculation with Bondarenko [5] self-shielding factors or effective cross sections derived from the probability tables with their own self-shielding factors. The

second route, cross section production, employed in this study, is actually our most applicable calculation. One needs to keep in mind that the effective cross section may strongly vary with dilution but also differentially from one channel to another.

Table 1 UR file 2 parameters interpretation

Evaluation	UR range (eV)	Points/decade	INT	LSSF	Shape
W-184	2.65E+03- 1.00E+05	3 / 2.5	5		lin-lin
U-233	6.00E+02- 4.00E+04	17	2	1	rough
U-238	2.00E+04- 1.49E+05	18	5	1	lin-lin, Gx
Pu-238	2.00E+02- 1.00E+04	constant			
Pu-239	2.50E+03- 3.00E+04	48	2		rough
Pu-240	5.70E+03- 4.00E+04	constant			

The following Figs. 2 to 5 show the computation from CALENDF and NJOY of probability tables derived effective cross sections at different dilutions, highlighting those differences and exemplifying the effects.

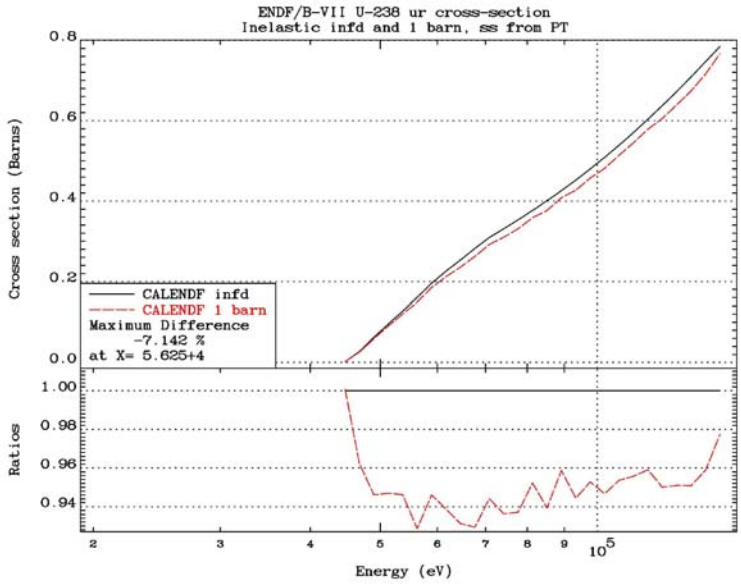

Figure 2 U-238 CALENDF inelastic effective cross section

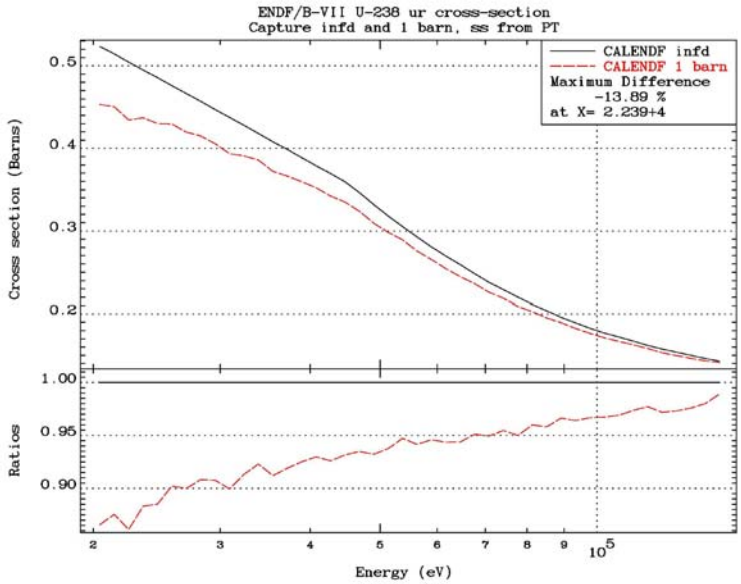

Figure 3 U-238 CALENDF capture effective cross section

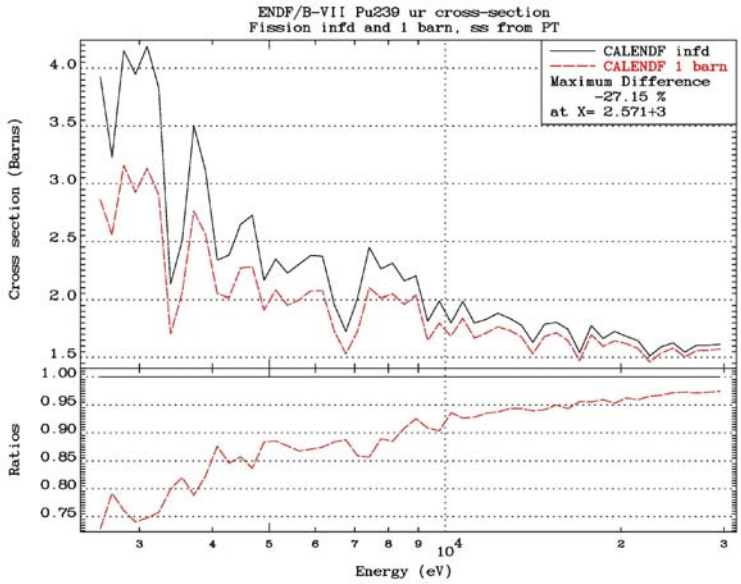

Figure 4 Pu239 CALENDF effective cross section

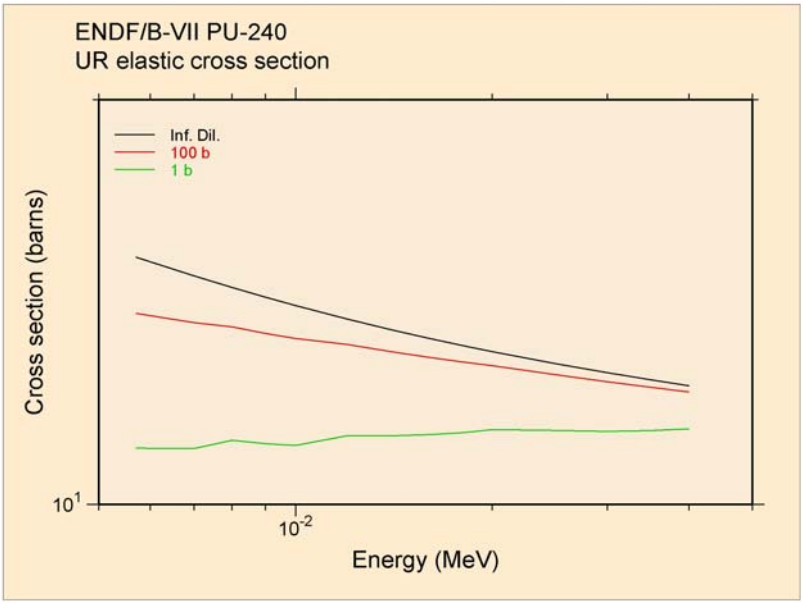

Figure 5 Pu240 NJOY effective cross section

In the U-238 the energy dependant self-shielding factors varies from 11, 13 and 5 % for respectively the elastic, capture and inelastic cross section in-between 20 to 150 KeV. For the Pu239 the same channels experience variation of 12, 32 and 0 % in-between the energies of 2.5 and 30 KeV.

3 Unresolved range parameters interpretations and formalism sensitivity

The unresolved resonance range treatment in ENDF has never been improved since it was defined in the 80's, and contains some ambiguities. The fact that only a single formalism is allowed, Single Level Breit-Wigner already caused some concern [10]. This is particularly true if differences are the results of altered resonance shapes or forbidden additional reactions, and not due merely to changes in the allowed underlying dilute-average cross sections.

In order to gain insight into the importance of the resonances shapes and depressions, and different formalisms, the following calculational benchmark has been devised. The CALENDF code has been modified to allow for a user choice of the formalism used in the unresolved resonance range. The choices include: Single Level Breit-Wigner, Multi Level Breit-Wigner, Breit-Wigner, and Reich Moore with a flag to set on and off accounting for external resonances. It should be understood that the original evaluation parameters are not modified in any way, just the way they are going to be interpreted is adapted. Modified ENDF/B-VII evaluations have been created with non-zero fission spectra only, in the unresolved resonance range of each isotope. This is done in order to isolate the effects of interest from differences in slowing down. It in fact maximizes the effect of resonances shapes.

When using the Monte Carlo code TRIPOLI [11] one can choose, or not, to sample CALENDF probability tables in and only the unresolved range of an evaluation. Without probability table sampling, the code access the smooth NJOY unresr data contained in the pointwise processed file. So for each "new" evaluation, one has a choice of four interpretations in and only the unresolved range that will be refer as:

MNBW = Multi Niveau Breit-Wigner CALENDF interpreted PT's
SLBW = Single Level Breit-Wigner CALENDF interpreted PT's
RM = Reich Moore CALENDF interpreted PT's
infd = no PT's, smooth NJOY unresr infinitely dilute cross section

A single geometry is used, a 30 cm sphere filled independently with two types of materials: H_2O (ENDF/B-VII) plus one isotope or the isotope alone. With 100 millions ($1.0x10^8$) histories and the Red-616 group structure, the neutron source is also been sample in a flat spectra within the unresolved range.

The results on U-238 with different formalism interpretation in the unresolved resonance range are show for a water sphere in Fig. 6 and a solid sphere in Fig. 7. It clearly demonstrates that, with respect to the fact that the parameters are identical, only their formalisms interpretations are different

- Whatever the formalism, the shape impact is negligible, when a moderator is present.
- In a solid fuel, large difference exists between results with and without probability treatments, and this whatever the formalism.

Other base fuels, U-235 and Pu239 and moderator Na and Carbon have also been studied leading to the same conclusions.

This demonstrates that in the unresolved resonance range, the formalism is not so important, but it needs to be accompanied by a probability table treatment in order to allow the transport code to better represent reality. This is said with the knowledge that only one probability code has been used in this study, and that other processing codes may interpret differently, as it will be shown later, the same data parameter file. The end results derived from them may differ slightly.

The impact of opening other, forbidden channels has not been assessed in this calculational benchmark.

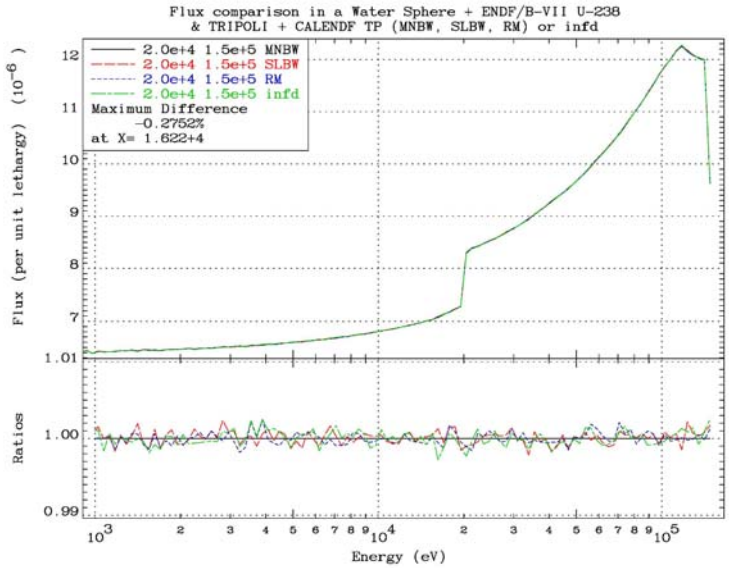

Figure 6 Water sphere neutron spectrum, S.D. 0.06% in the UR

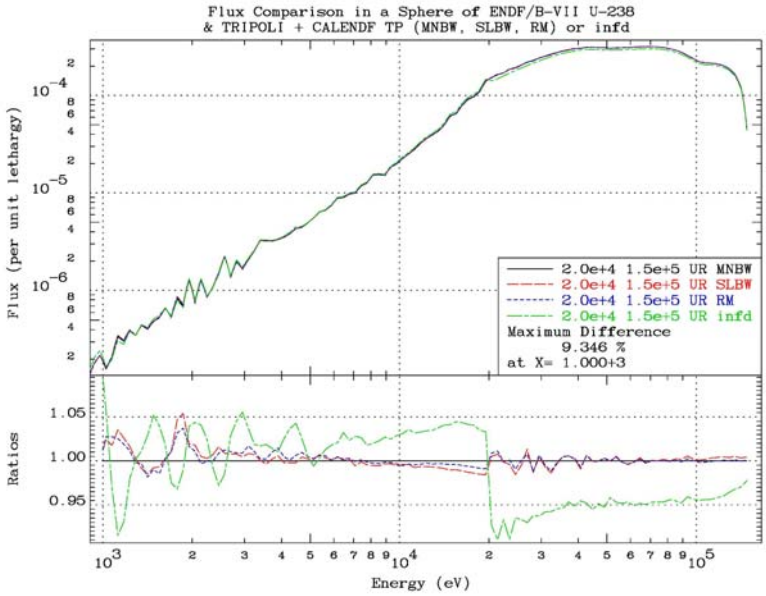

Figure 7 Solid sphere neutron spectrum, S.D. < 0.3% in the UR

4 Methods used by CALENDF

The code works with a set of energy groups defined across an energy range, in the unresolved resonance range (URR). Based on the average resonance parameters and the required accuracy, CALENDF defines energy zones adapted to the group structure. A 616 group structure, 50 bins per energy decades, equally spaced in the log of energy between, 10^{-5} and 20 MeV, coded Red-616 (Appendix A), is used in this study. If the group structure is coarse, several discontinuous zones are selected. If the structure is fine, a zone may cover several groups. Average parameters are computed for each zone using file 2 of the evaluation. Random ladders of resonances are generated with energies extracted from a table of 1185 values that are the eigenvalues of a random matrix (Dyson and Mehta) and with resonance widths chosen from the distribution laws with stratified and antithetic sampling. A few resonances are added below and above the range of the energy zone to handle edge effects.

The cross sections for each ladder are computed on a fine energy grid using the MNBW formalism (Multi Niveau Breit-Wigner, MNBW, is a slightly modified Multi Level Breit-Wigner treatment) and psi-chi Doppler broadening. There are no normalizations done except for the cases with LSSF=1. The moments of these cross-sections are computed, and the probability tables deduced from them. The table orders will mainly depend on the required accuracy, with a maximum of 11. The probability tables for all zones and ladders are merged to get the final table for each energy group. The Gauss-quadrature mathematical principle gives those probability tables their sturdiness, allowing many utilitarian operations such as table condensation, isotope mixing, or interpolation.

Figs. 8 and 9 illustrate some features of the performance of the CALENDF methods when generating resonant pointwise cross section in the unresolved range of an evaluation and comparing it with the NJOY unresr module results; smoothed averaged structure against statistically generated resonances. Below, in the resolved resonance range or above in the continuum, both codes lead to the same cross section levels.

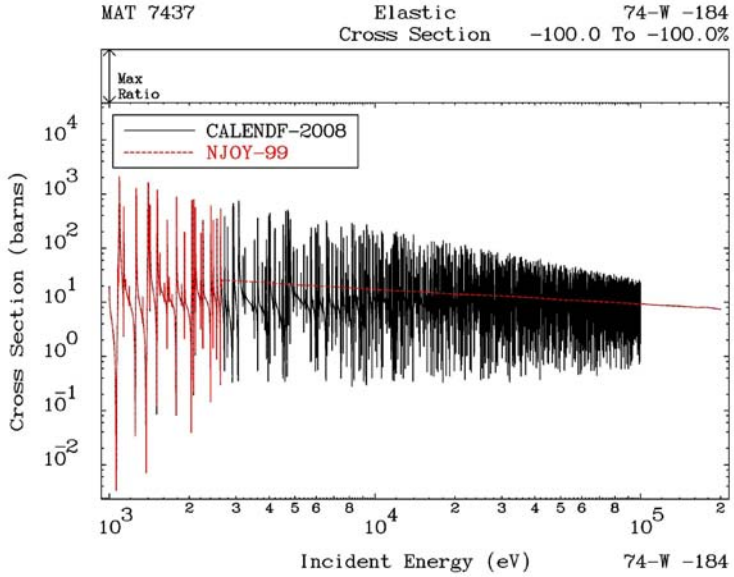

Figure 8 CALENDF - NJOY pointwise data in the UR

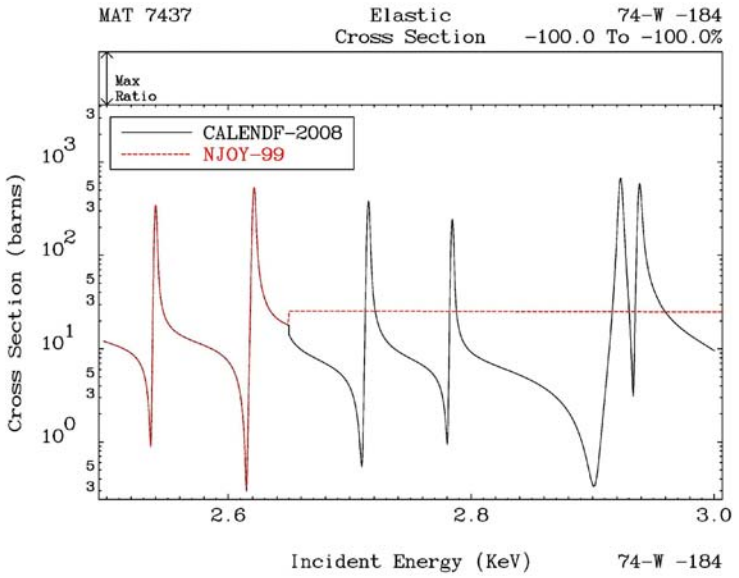

Figure 9 NJOY - CALENDF "statistical" resonance in the UR

In Figs. 10 and 11, showing W-194 elastic and capture cross sections, the large oscillations in the CALENDF probability table derived effective cross sections are caused by using definite group bounds for each sampling step, in this case 616 groups. The oscillations amplitudes are different from one channel; elastic with up to 40%, to another; capture with only 20%. They gradually go away when more ladders are averaged in (from 4 to 128 ladders) or when approaching the continuum, and integral results becomes reasonable, even with the statistical oscillations in the detailed cross sections. An optimum number of 16 ladders, for a cross section reconstruction accuracy of 0.02% has been assessed and used in this study.

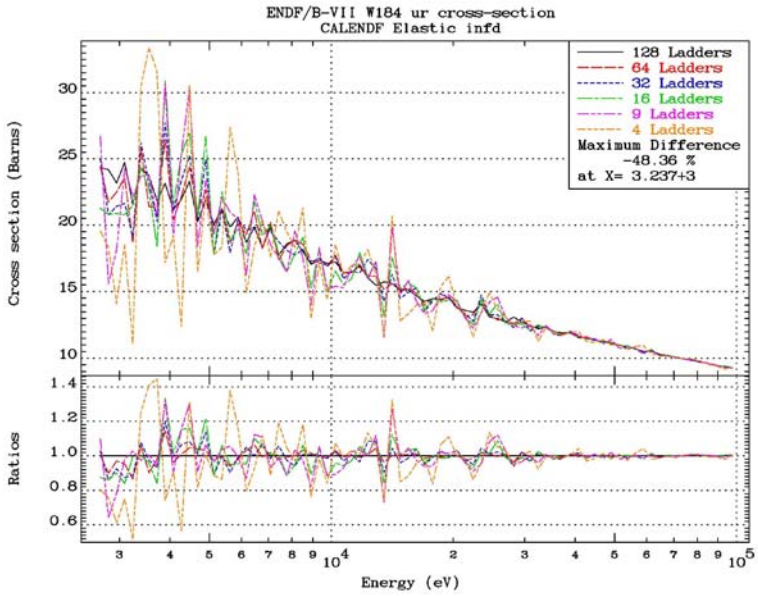

Figure 10 CALENDF ladders parametric study on elastic

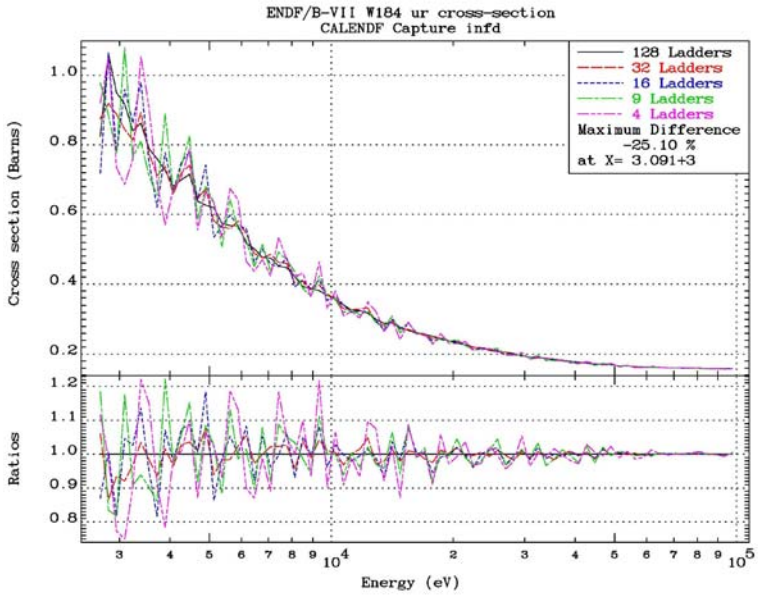

Figure 11 CALENDF ladders parametric study on capture

However, it ought to be said that even if one can see a better, more physically eye-pleasing agreement with 16 ladders and of course with the results of the other codes as well, this may still conceal problems. A code adopting a Gaussian orthogonal ensemble (GOE) to characterize the distribution of resonance energies (in contrast to a Wigner distribution) and using a single, well stratified, random sampling may be more realistic.

5 Effective cross sections comparisons

Here are comparisons of the results from four different processing codes; NJOY-PURR, CALENDF, AUROX and PURM on the six evaluations described in Table I. Those isotopes have been chosen to encompass most cases encountered in the unresolved energy range of any ENDF/B-VII or JEFF-3.1.1 evaluations. In a major library, like ENDF/B-VII containing 393 isotopes, it is interesting to account for the fact that 252 of them have a declared unresolved energy range (140 for JEFF-3.1.1). The minimum energy encountered for an unresolved range is 1 eV and the maximum is 1 MeV.

What was asked of the participants were all unresolved range cross-sections in the unresolved range of those six ENDF/B-VII evaluations, at 293.6 Kelvin, both infinitely dilute, and 1 barns, in simple 2E11.4 column format. However simple this may seem, it took quite a few iterations to finalize the series of graphs in this section.

To understand the differences it is useful to summarize the methods used for the unresolved resonances range in the various codes, but for CALENDF used as a reference, not a standard, which methods have already been described.

5.1 Summary of the methods used in NJOY

The probability tables are generated using the PURR module of NJOY [5]. For each energy given in the evaluation, the parameters for a long series (or "ladder") of resonances are constructed using Wigner spacing for resonance centers and the chi-squared distributions from the evaluation for resonance widths. The code then randomly selects an energy in the range of the series and computes the cross sections at that point using Single-Level Breit-Wigner (SLBW) resonance shapes and psi-chi Doppler broadening. In the beginning, it does this for a number of random energies to get a rough idea of the distribution of the total cross section; it then analyzes this rough idea to construct a set of total cross section bins for the rest of the process (typically, 20 bins are used). It then returns to the first ladder and samples it with random energies. The resulting total cross sections are added to the appropriate bin in the probability table, and the conditional averages for scattering, fission, and capture are accumulated in the bin corresponding to the total cross section. The code then constructs a new ladder and repeats the sampling process. This is continued for the requested number of ladders (in this case study 128). For materials with the ENDF LSSF parameter set to zero, the table cross sections are renormalized to match the computed infinitely dilute values. For LSSF=1, the values in the table are converted to self shielding factors, and then transport code multiplies these factors times the cross sections from the standard ENDF file to get the appropriate value. Note that there are no energy bounds (such as group bounds) in this process. Therefore, it computes cross sections that have basically the same smoothness as the unresolved resonance range evaluation.

5.2 Summary of the methods used in AUROX

The unresolved resonance processing code, AUROX [6], uses the ladder method, but with unoptimized standard bins, some of which are always empty during the ladder sampling process. Cross sections are computed from the SLBW parameters and Doppler broadened

with the psi-chi method. Ladder sampling continues until the statistical convergence of the resonance components of the average total, elastic, fission, and capture cross sections (2%), or when 500 ladders have been sampled. Each table is then collapsed to 20 bins whose boundaries are optimized on equal probabilities. In the transport code, elastic, capture, and fission cross sections are treated using conditional means, i.e., a total cross section sampled from a table is associated with a set of mean partial cross sections. The LSSF parameter determines whether the cross sections sampled from the table are added to the file 3 data or used as self-shielding factors.

5.3 Summary of the methods used in PURM

PURM (Probability tables for the Unresolved Region using Monte Carlo) [7] is a module that uses a Monte Carlo approach to calculate probability tables on an evaluator-defined energy grid in the unresolved-resonance region (URR). For each probability table, PURM samples pairs of resonances surrounding the reference energy. The resonance distribution is sampled for each spin sequence (i.e., L-J pair), and PURM uses the Dyson and Mehta Δ_3 statistics test to determine the number of resonances to sample for each spin sequence. For each resonance, PURM samples the resonance widths from a Chi-square distribution for a specified number of degrees of freedom. Once the resonance parameters are sampled, PURM calculates the total, capture, fission and scatter cross sections at the reference energy using the Single-level Breit-Wigner formalism with appropriate treatment for temperature effects. The energy cross-section calculation constitutes a single iteration or history. For the cross-section calculation and corresponding probability-table calculation, PURM processes a user-specified number of batches with a corresponding number of histories per batch. For each history, PURM calculates the total, capture, fission, competitive reaction and scatter cross section at the reference energy, and the corresponding contribution to the capture, fission, scattering and competitive reaction probability table is determined for each history. Total is re-calculated as sum of partial reactions including inelastic given as competitive. After completing the specified number of histories for a batch, a batch estimate for the probability for each cross-section band within a table is obtained by dividing the number of tallies for the band by the total number of histories processed. Additional batches are processed until the user-specified number of batches is complete. Due to the nature of the calculational procedures, PURM provides a mechanism for monitoring the convergence of the cross-section calculation. For each reaction, a plot of the calculated cross section is provided by batches run.

The resulting cross sections in the probability table are renormalized such that the average value of a cross section (total, fission, capture, elastic and competition) is equal to the infinite dilute value for that cross section.

5.4 Pu238 UR cross sections

The next figures show the comparison of effective cross sections, total, elastic, capture and fission infinitely dilute, then at 1 barn for the 4 codes. It shows the unacceptably large differences that can occur when the processing codes interpolate the cross section (PURM, AUROX) in-between the evaluator given energy grid or the parameters (NJOY, CALENDF). In this particular case, the self- shielded cross sections show some significant differences not all well understood. Earlier anomalous results for capture have been traced to an obscure code bug in AUROX, now corrected. We believe this kind of inter-comparison is very useful because it highlights both processing code bugs and the effects of modeling differences.

Figure 12 Pu238 UR cross section comparison – 4 codes

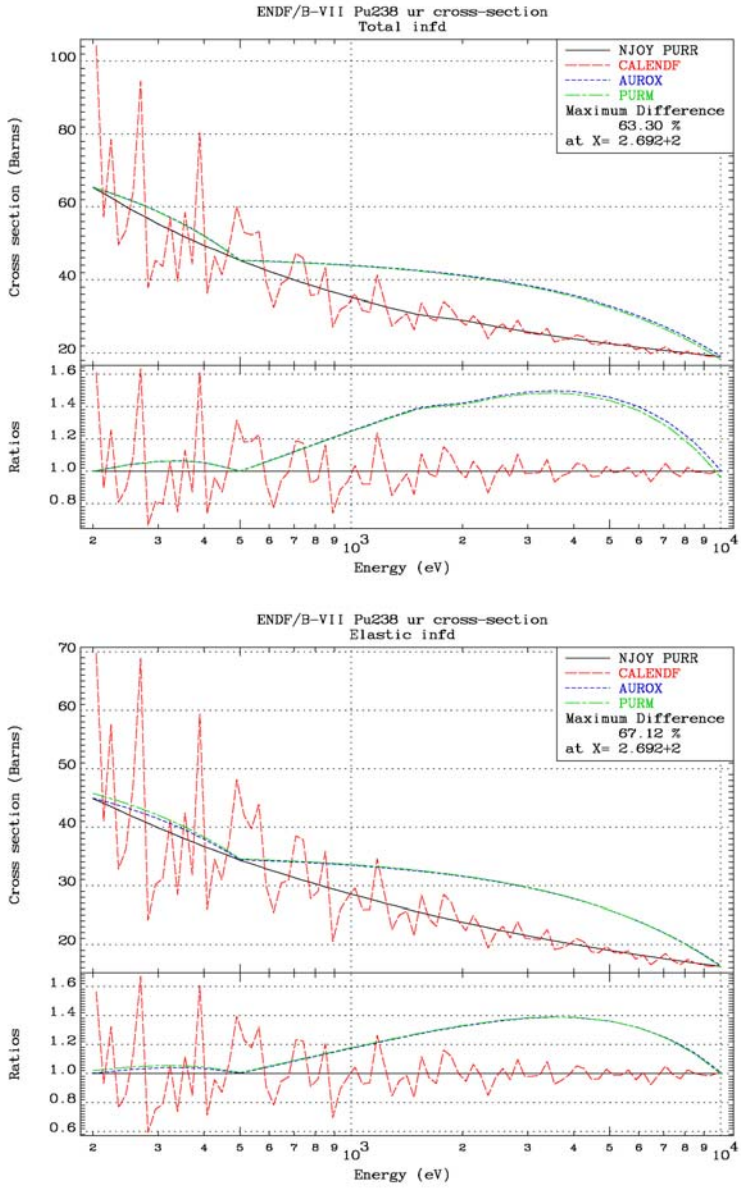

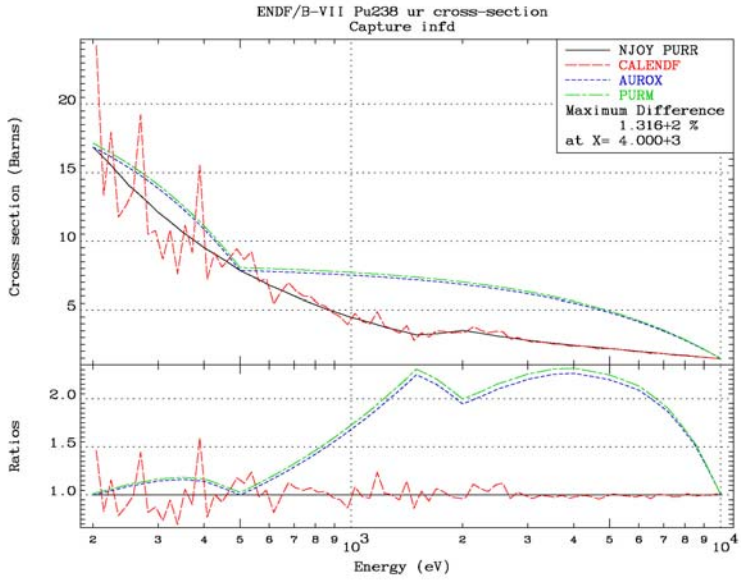
ENDF/B-VII Pu238 ur cross-section
Capture infd
NJOY PURR
CALENDF
AUROX
PURM
Maximum Difference
1.316+2 %
at X= 4.000+3
Cross section (Barns)
Ratios
Energy (eV)

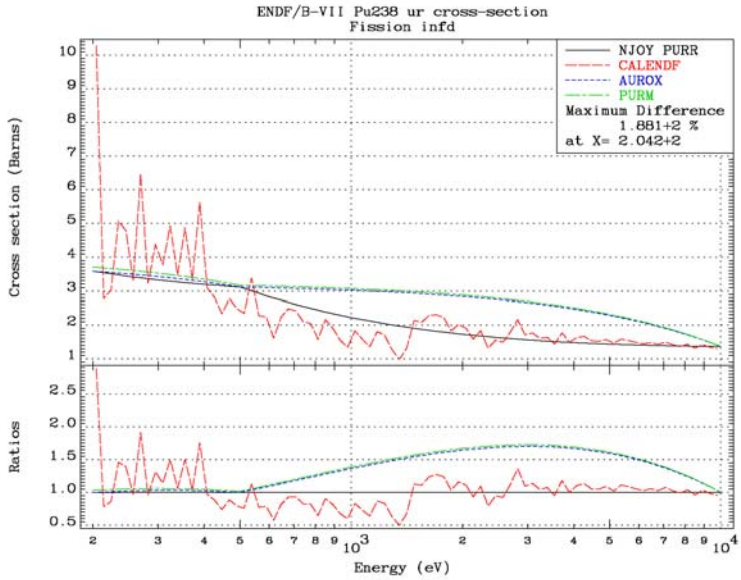
ENDF/B-VII Pu238 ur cross-section
Fission infd
NJOY PURR
CALENDF
AUROX
PURM
Maximum Difference
1.881+2 %
at X= 2.042+2
Cross section (Barns)
Ratios
Energy (eV)

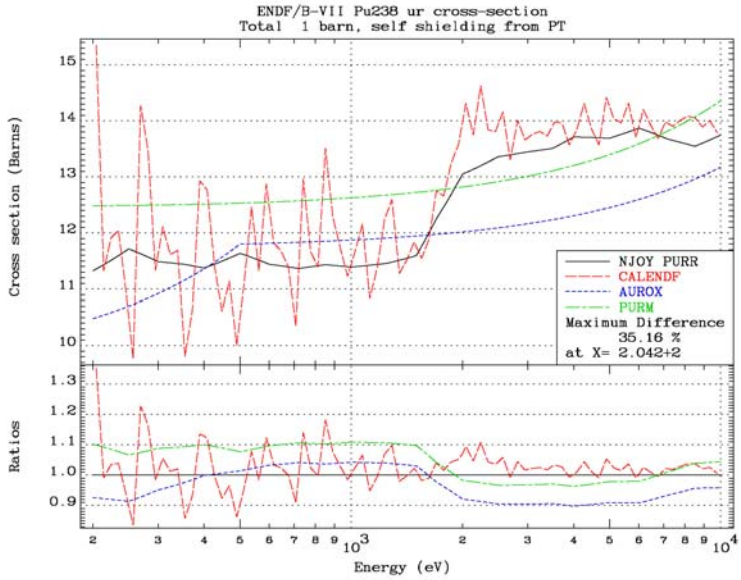
ENDF/B-VII Pu238 ur cross-section
Total 1 barn, self shielding from PT
NJOY PURR
CALENDF
AUROX
PURM
Maximum Difference
35.16 %
at X= 2.042+2
Cross section (Barns)
Ratios
Energy (eV)

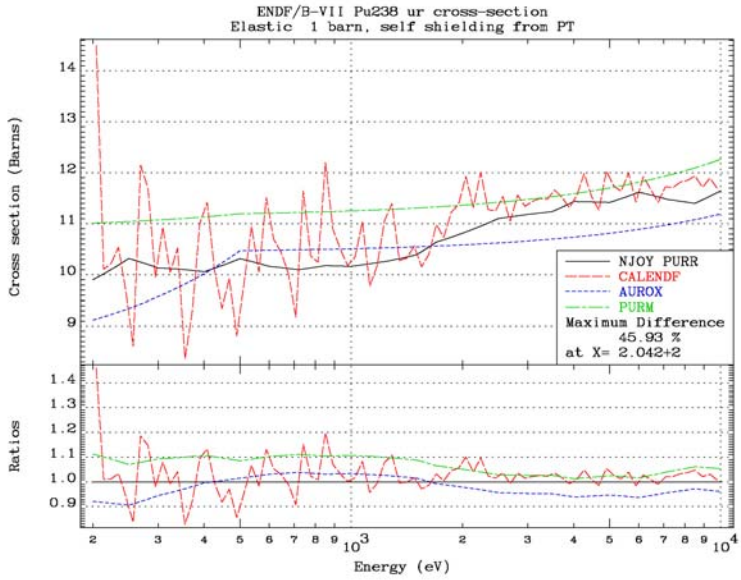
ENDF/B-VII Pu238 ur cross-section
Elastic 1 barn, self shielding from PT
Cross section (Barns)
NJOY PURR
CALENDF
AUROX
PURM
Maximum Difference
45.93 %
at X= 2.042+2
Ratios
Energy (eV)

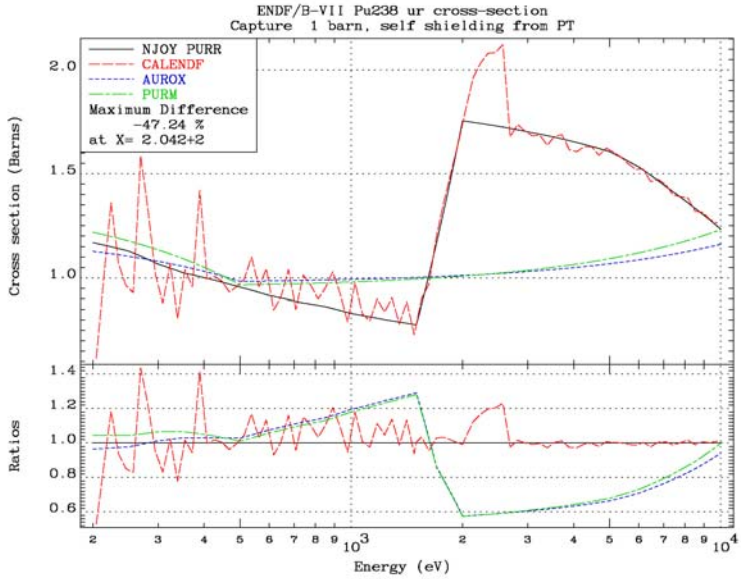
ENDF/B-VII Pu238 ur cross-section
Capture 1 barn, self shielding from PT
Cross section (Barns)
NJOY PURR
CALENDF
AUROX
PURM
Maximum Difference
-47.24 %
at X= 2.042+2
Ratios
Energy (eV)

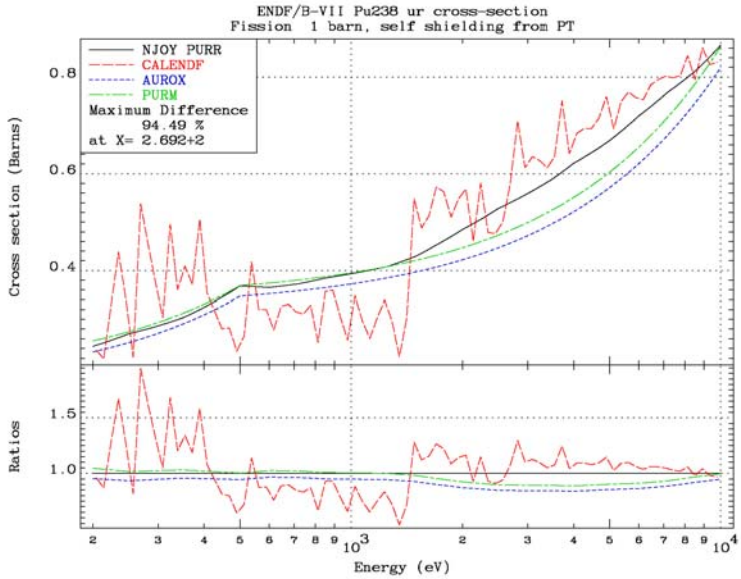
ENDF/B-VII Pu238 ur cross-section
Fission 1 barn, self shielding from PT
Cross section (Barns)
NJOY PURR
CALENDF
AUROX
PURM
Maximum Difference
94.49 %
at X= 2.692+2
Ratios
Energy (eV)

5.5 Pu239 UR cross sections

The next figures show the comparison of effective cross sections, total, elastic, capture and fission infinitely dilute, then at 1 barn for the 4 codes. A much better agreement than previously can be seen in the infinitely dilute cross section. AUROX was missing the 3.55 KeV data point but was corrected during this study and this was leading to a peaked 17.7% differences. CALENDF methods tend to smooth averages across a band that includes the rough 100 eV width parameters given in the file 2. Those large step fluctuations, qualified as gross structures by the evaluator raise some questions on their validity and concern over their interpretation. The above 8 KeV differences can be trace back to the presence of an MF-3, MT-51, inelastic level that is only accounted for in the CALENDF probability tables, but then not shelf-shielded. MF-3 cross section can be read independently from file two, although care should then be taken in calculating the total. Here again the PURM 1 barn self-shielded cross section departs from results of the others codes.

Figure 13 Pu239 UR cross section comparison – 4 codes

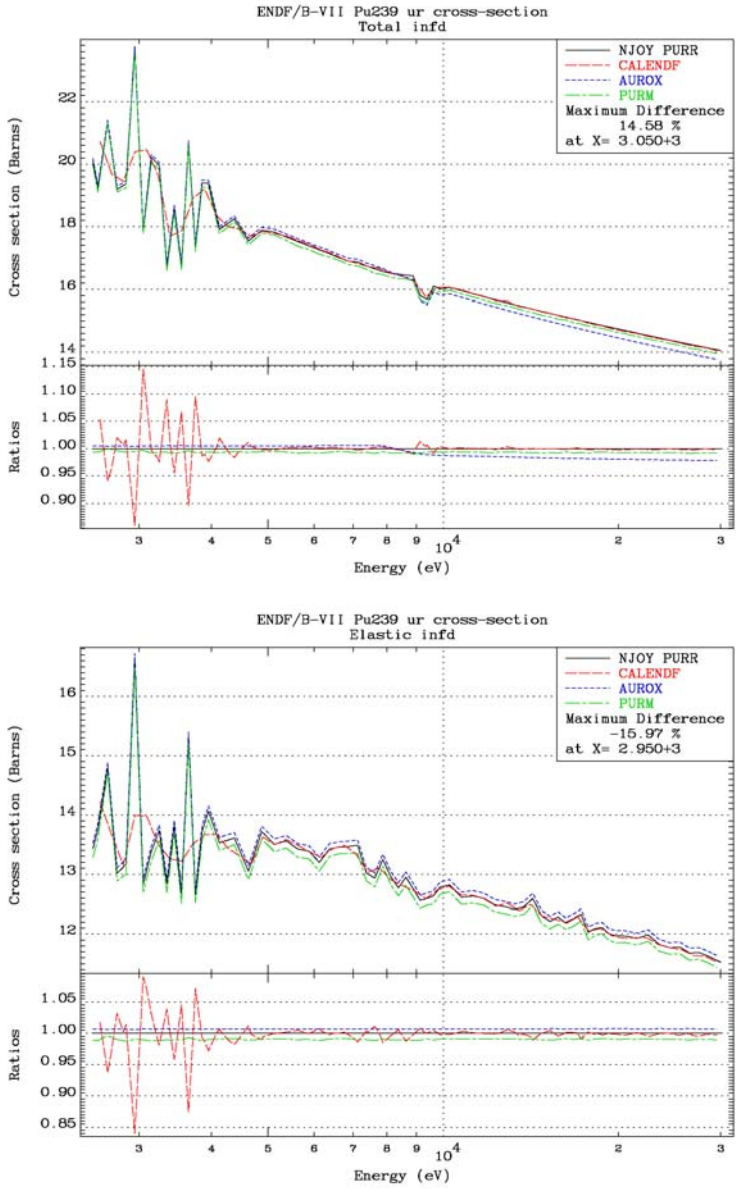

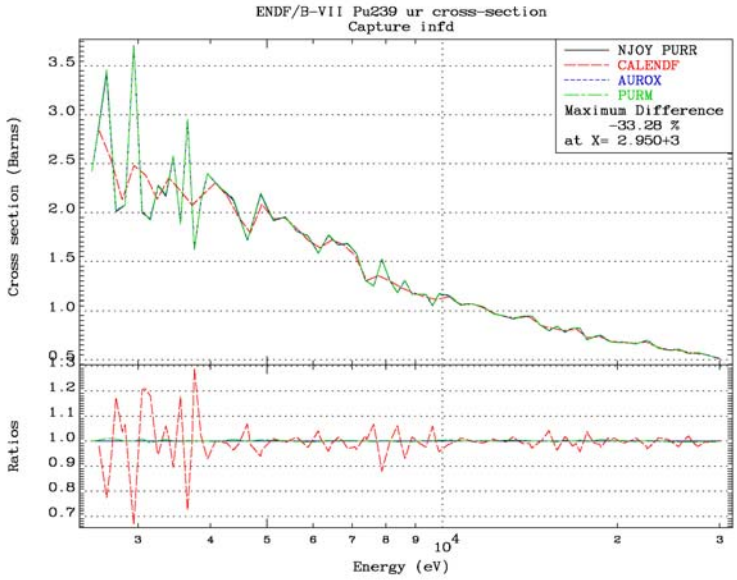
ENDF/B-VII Pu239 ur cross-section
Capture infd
NJOY PURR
CALENDF
AUROX
PURM
Maximum Difference
-33.28 %
at X= 2.950+3
Cross section (Barns)
Ratios
Energy (eV)

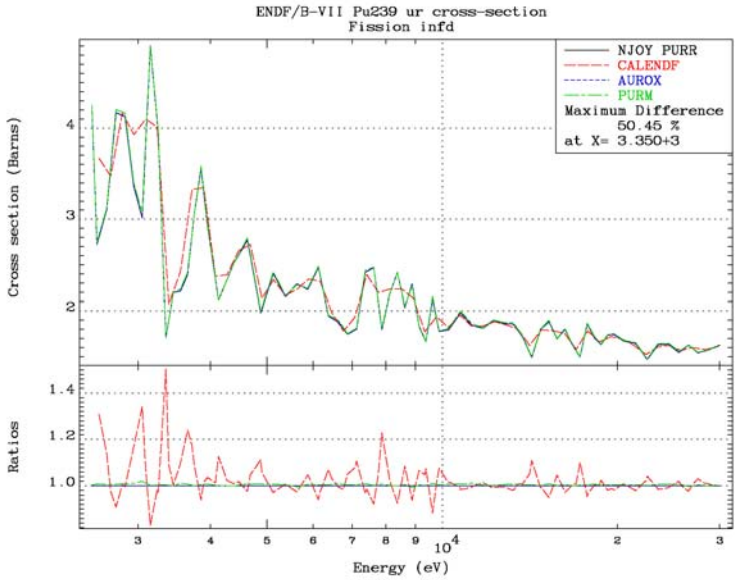
ENDF/B-VII Pu239 ur cross-section
Fission infd
NJOY PURR
CALENDF
AUROX
PURM
Maximum Difference
50.45 %
at X= 3.350+3
Cross section (Barns)
Ratios
Energy (eV)

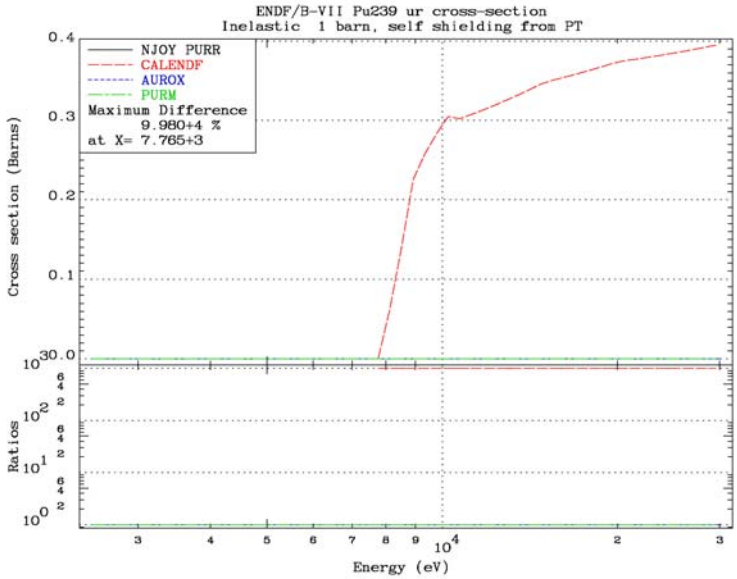
ENDF/B-VII Pu239 ur cross-section
Inelastic 1 barn, self shielding from PT
NJOY PURR
CALENDF
AUROX
PURM
Maximum Difference
9.980+4 %
at X= 7.765+3
Cross section (Barns)
Ratios
Energy (eV)

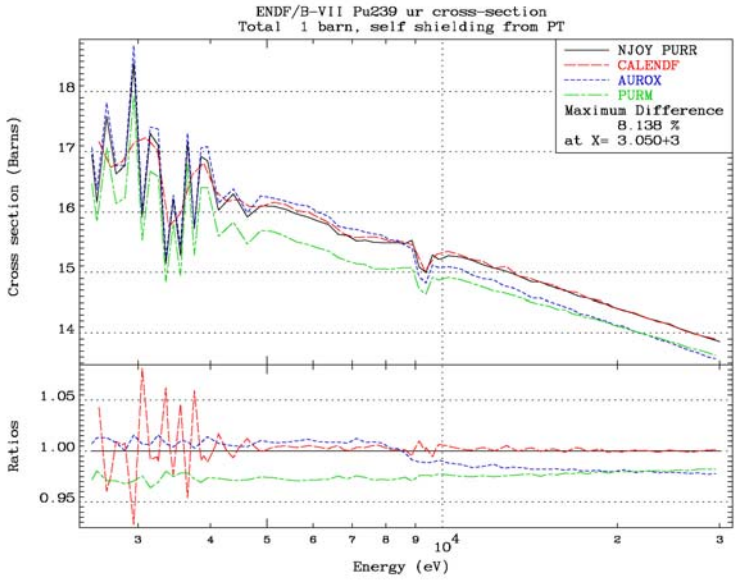
ENDF/B-VII Pu239 ur cross-section
Total 1 barn, self shielding from PT
NJOY PURR
CALENDF
AUROX
PURM
Maximum Difference
8.138 %
at X= 3.050+3
Cross section (Barns)
Ratios
Energy (eV)

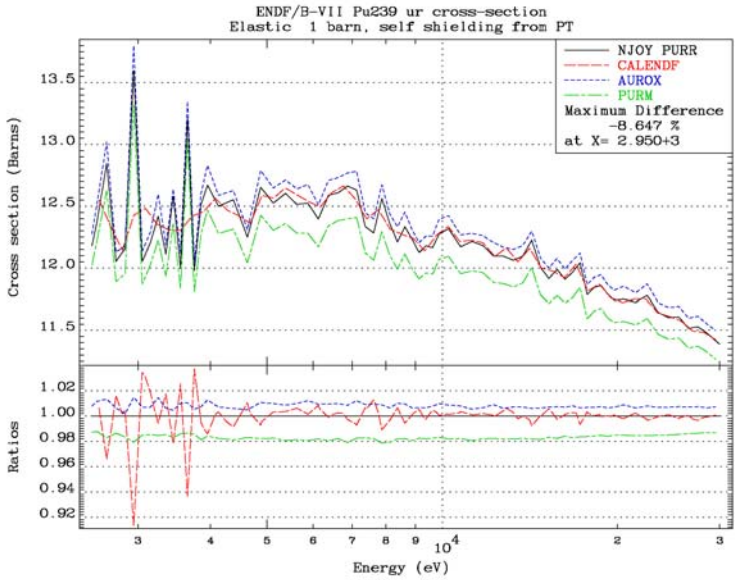
ENDF/B-VII Pu239 ur cross-section
Elastic 1 barn, self shielding from PT
NJOY PURR
CALENDF
AUROX
PURM
Maximum Difference
-8.647 %
at X= 2.950+3
Cross section (Barns)
Ratios
Energy (eV)

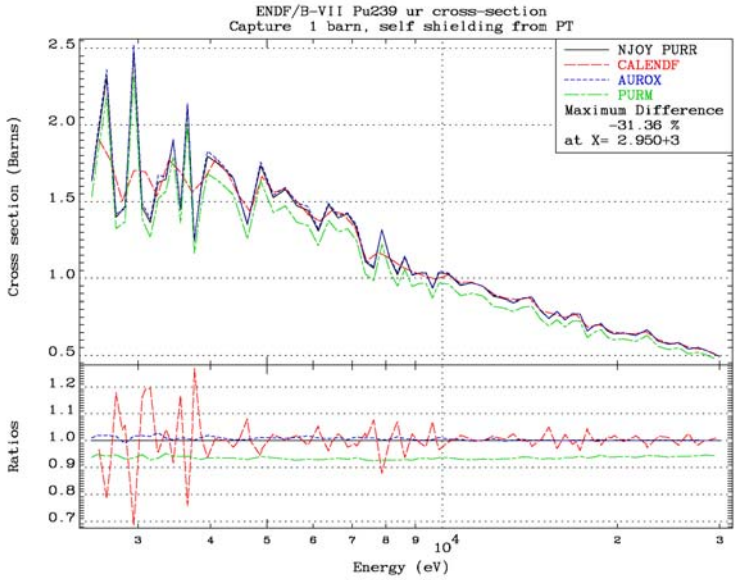
ENDF/B-VII Pu239 ur cross-section
Capture 1 barn, self shielding from PT
NJOY PURR
CALENDF
AUROX
PURM
Maximum Difference
-31.36 %
at X= 2.950+3
Cross section (Barns)
Ratios
Energy (eV)

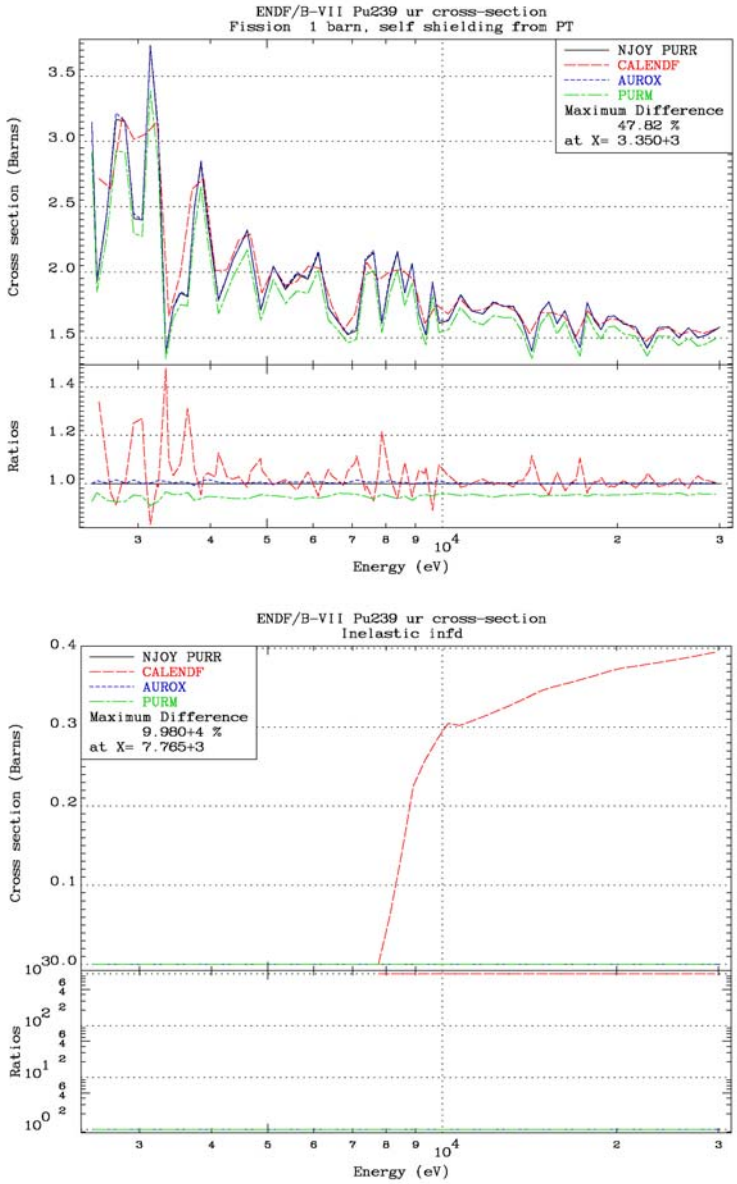

Even for CALENDF, the inelastic channel read from file 3 cannot be shelf-shielded because there are no Γ_x in the file 2. However, nothing would prohibit using the self-shielding factors of the total to account for it.

5.6 Pu240 UR cross sections

An even much nicer agreement is seen on the infinitely dilute unresolved resonance range cross section for this isotope, in line with what ought to be expected. Earlier 1 barn PURM results departed by values ranging from 20 to 30% from results of the other codes, however the code has been corrected in the course of this study, making the comparison more reasonable.

Figure 14 Pu240 UR cross sections comparison – 4 codes

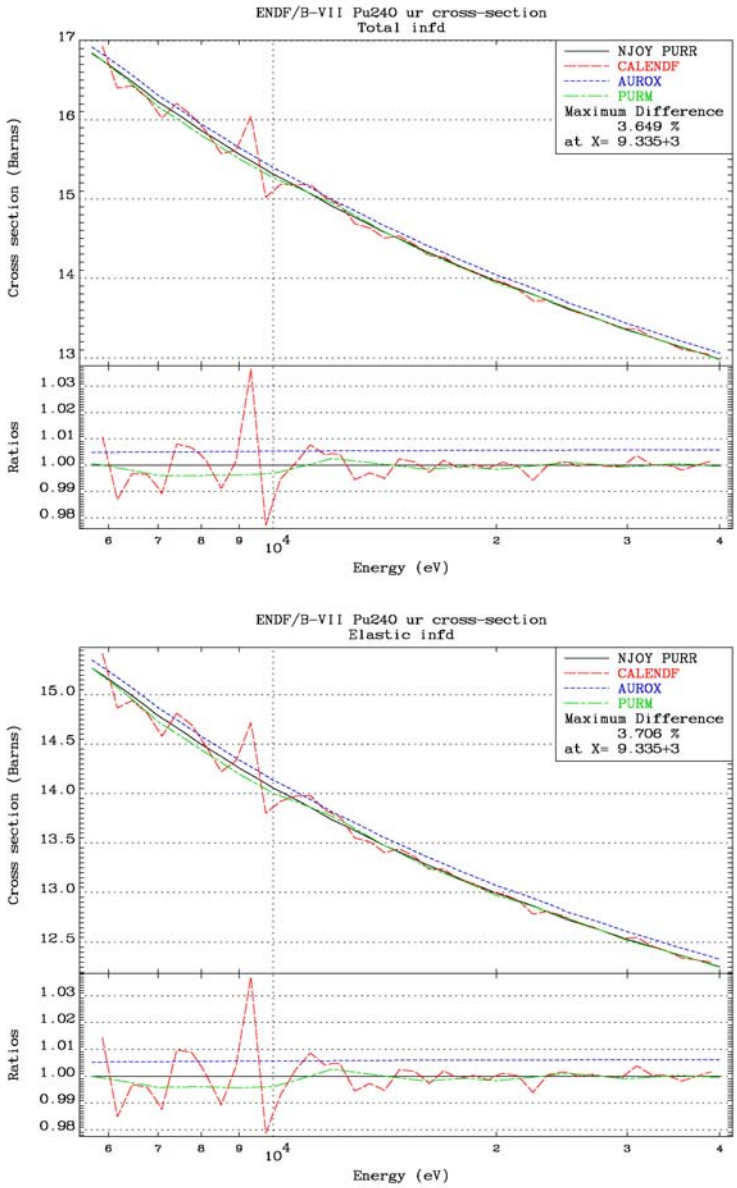

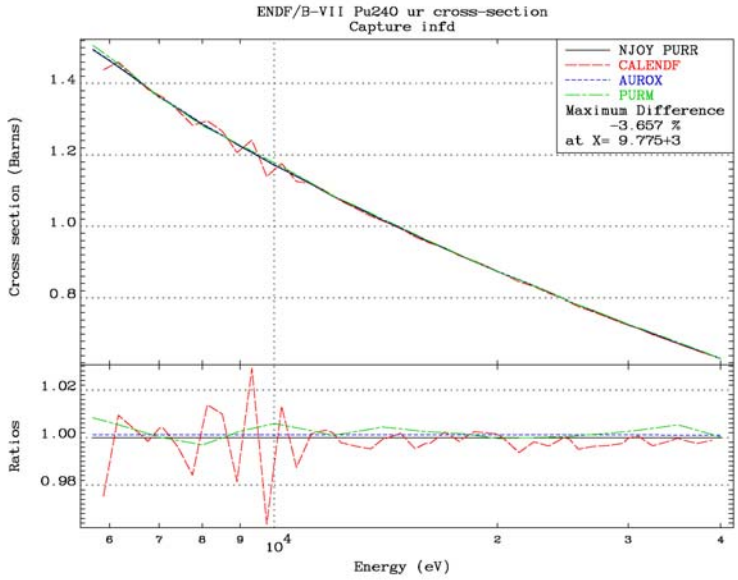
ENDF/B-VII Pu240 ur cross-section
Capture infd
NJOY PURR
CALENDF
AUROX
PURM
Maximum Difference
-3.657 %
at X= 9.775+3
Cross section (Barns)
Ratios
Energy (eV)

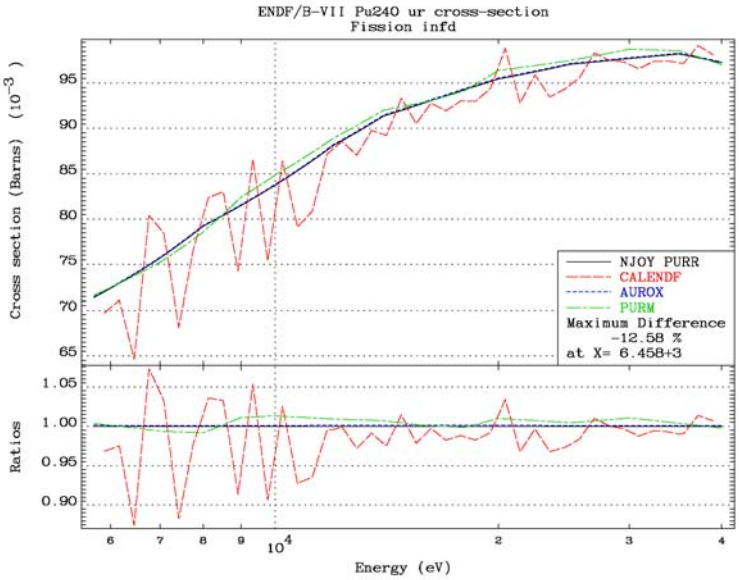
ENDF/B-VII Pu240 ur cross-section
Fission infd
NJOY PURR
CALENDF
AUROX
PURM
Maximum Difference
-12.58 %
at X= 6.458+3
Cross section (Barns) (10^-3)
Ratios
Energy (eV)

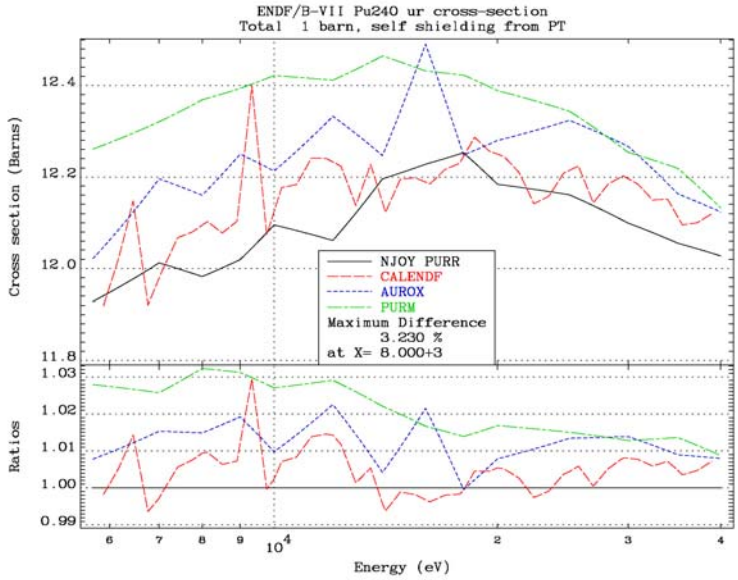
ENDF/B-VII Pu240 ur cross-section
Total 1 barn, self shielding from PT
NJOY PURR
CALENDF
AUROX
PURM
Maximum Difference
3.230 %
at X= 8.000+3
Cross section (Barns)
Ratios
Energy (eV)

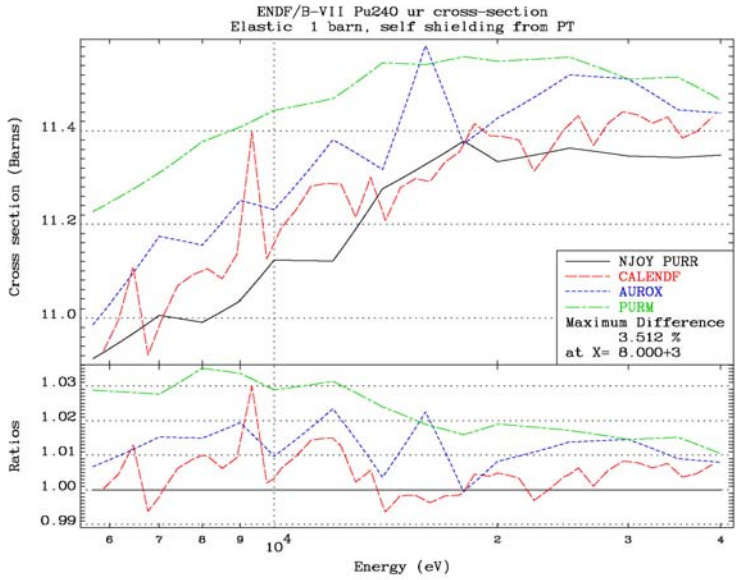
ENDF/B-VII Pu240 ur cross-section
Elastic 1 barn, self shielding from PT
Cross section (Barns)
11.4
11.2
11.0
NJOY PURR
CALENDF
AUROX
PURM
Maximum Difference
3.512 %
at X= 8.000+3
Ratios
1.03
1.02
1.01
1.00
0.99
6 7 8 9 10^4 2 3 4
Energy (eV)

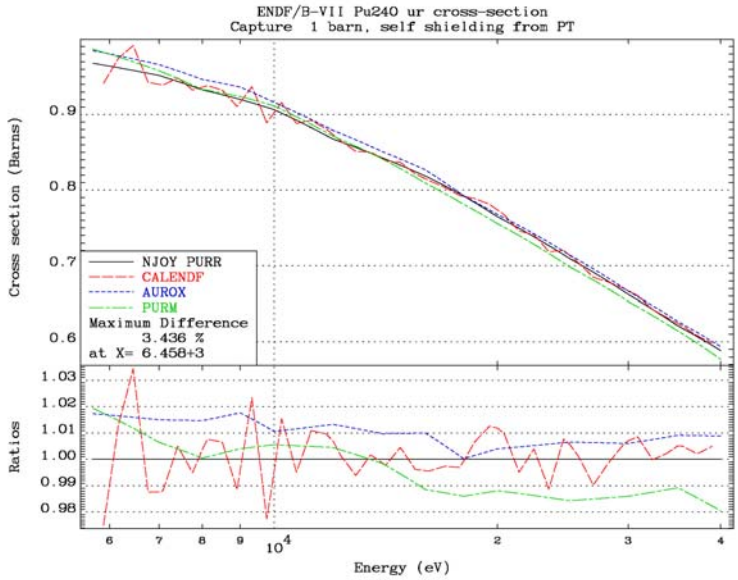
ENDF/B-VII Pu240 ur cross-section
Capture 1 barn, self shielding from PT
Cross section (Barns)
0.9
0.8
0.7
0.6
NJOY PURR
CALENDF
AUROX
PURM
Maximum Difference
3.436 %
at X= 6.458+3
Ratios
1.03
1.02
1.01
1.00
0.99
0.98
6 7 8 9 10^4 2 3 4
Energy (eV)

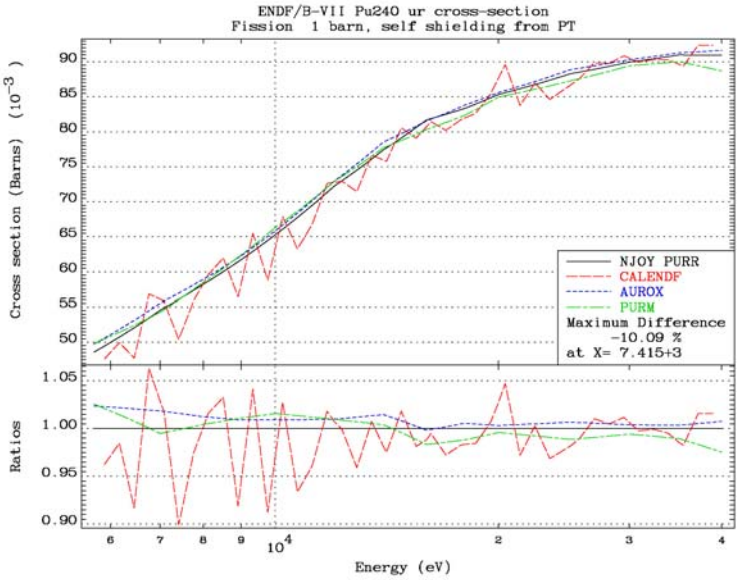
ENDF/B-VII Pu240 ur cross-section
Fission 1 barn, self shielding from PT
Cross section (Barns) (10^-3)
90
85
80
75
70
65
60
55
50
NJOY PURR
CALENDF
AUROX
PURM
Maximum Difference
-10.09 %
at X= 7.415+3
Ratios
1.05
1.00
0.95
0.90
6 7 8 9 10^4 2 3 4
Energy (eV)

5.7 U-233 UR cross sections

This is the first of the two LSSF=1 evaluations considered here, in which the cross sections are given in file 3 and should not be computed. As expected, only negligible differences occur with CALENDF results plotted on a group structure different from the energy grid at which the cross sections are given. Self shielded 1 barn cross section comparison also agree remarkably well but for the PURM results that can derive by up to 20%.

Figure 15 U-233 UR cross sections comparison - 4 codes

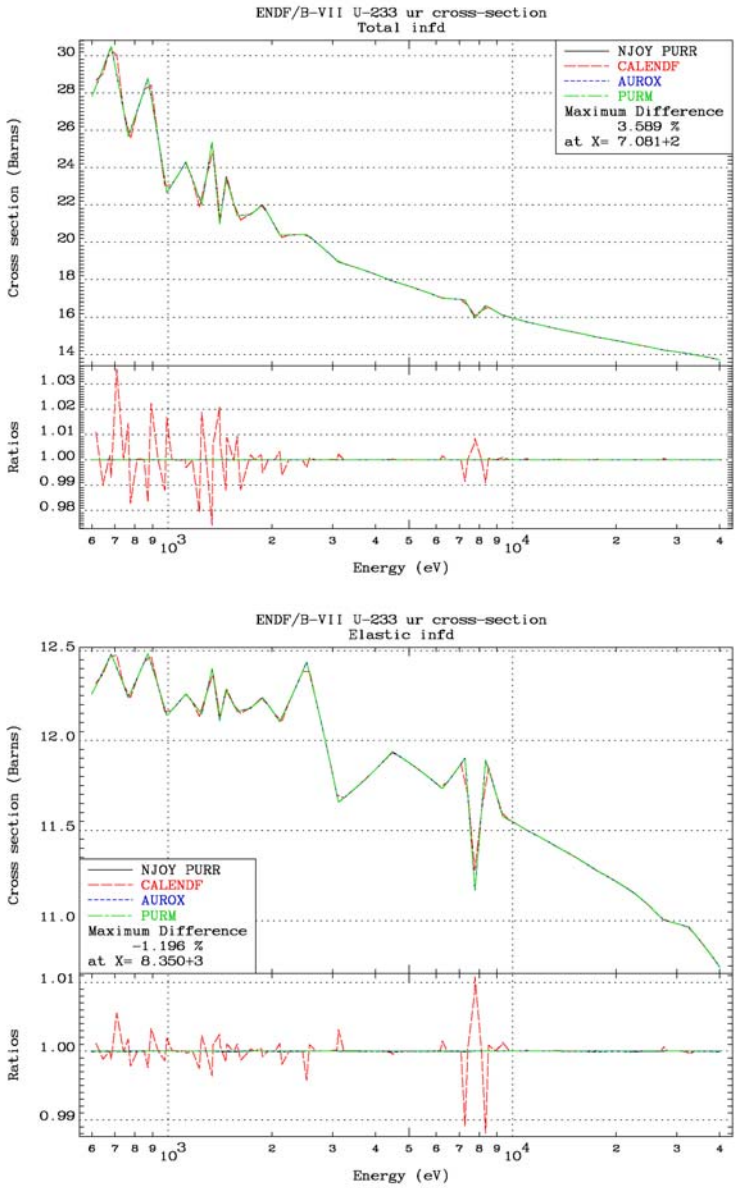

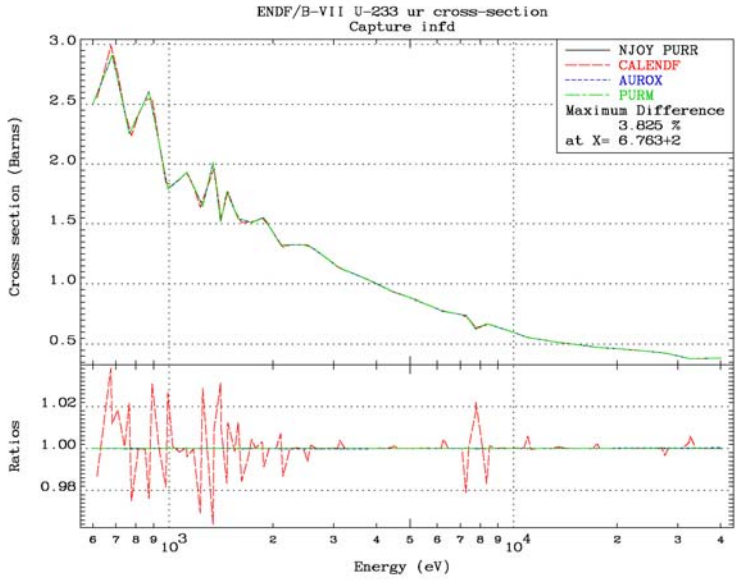
ENDF/B-VII U-233 ur cross-section
Capture infd
NJOY PURR
CALENDF
AUROX
PURM
Maximum Difference
3.825 %
at X= 6.763+2
Cross section (Barns)
Ratios
Energy (eV)

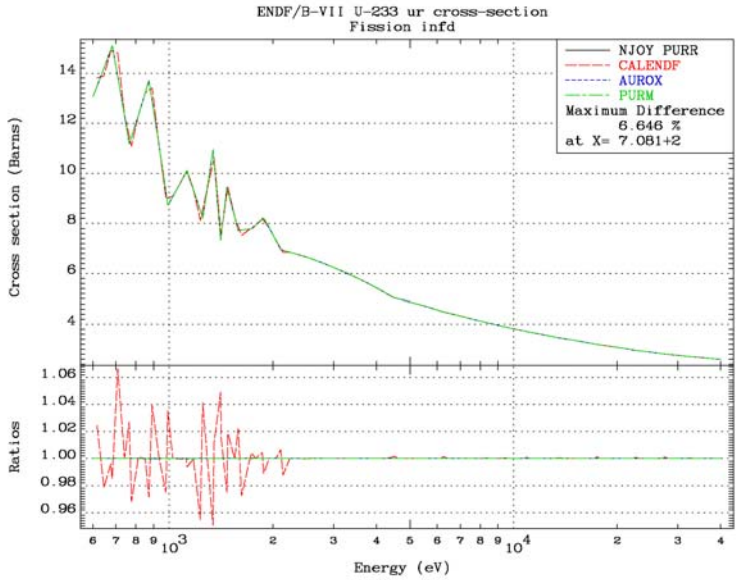
ENDF/B-VII U-233 ur cross-section
Fission infd
NJOY PURR
CALENDF
AUROX
PURM
Maximum Difference
6.646 %
at X= 7.081+2
Cross section (Barns)
Ratios
Energy (eV)

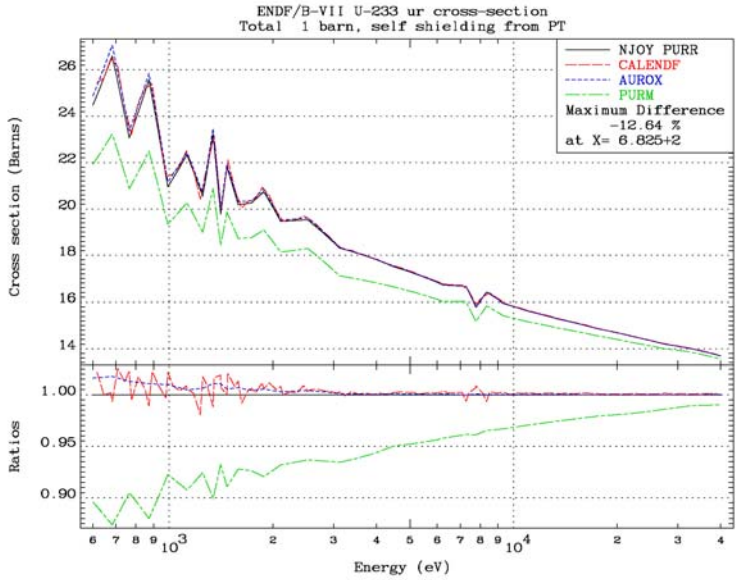
ENDF/B-VII U-233 ur cross-section
Total 1 barn, self shielding from PT
NJOY PURR
CALENDF
AUROX
PURM
Maximum Difference
-12.64 %
at X= 6.825+2
Cross section (Barns)
Ratios
Energy (eV)

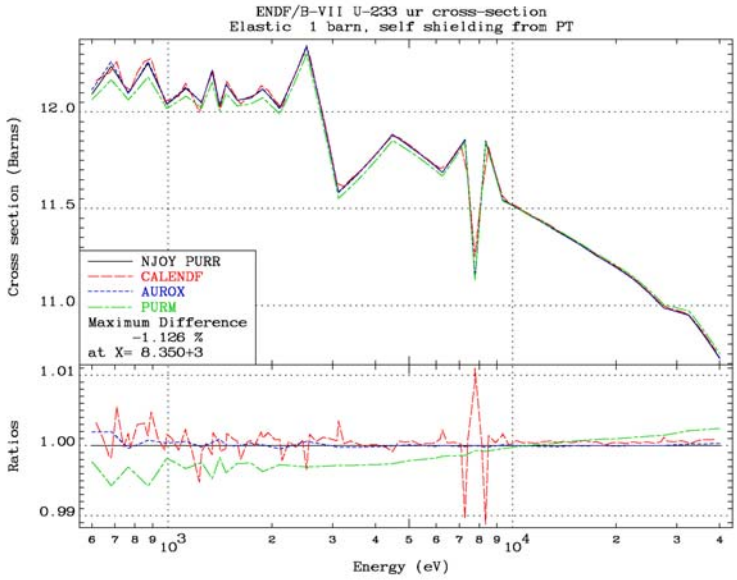
ENDF/B-VII U-233 ur cross-section
Elastic 1 barn, self shielding from PT
Cross section (Barns)
NJOY PURR
CALENDF
AUROX
PURM
Maximum Difference
-1.126 %
at X= 8.350+3
Ratios
Energy (eV)

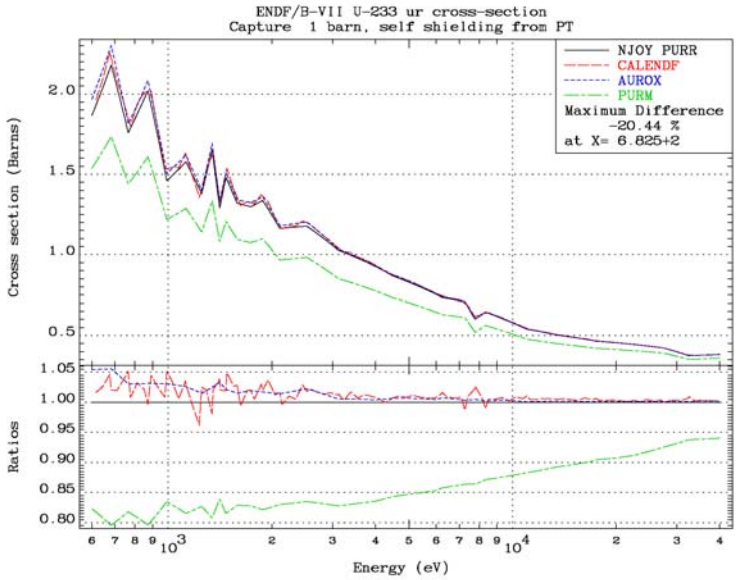
ENDF/B-VII U-233 ur cross-section
Capture 1 barn, self shielding from PT
Cross section (Barns)
NJOY PURR
CALENDF
AUROX
PURM
Maximum Difference
-20.44 %
at X= 6.825+2
Ratios
Energy (eV)

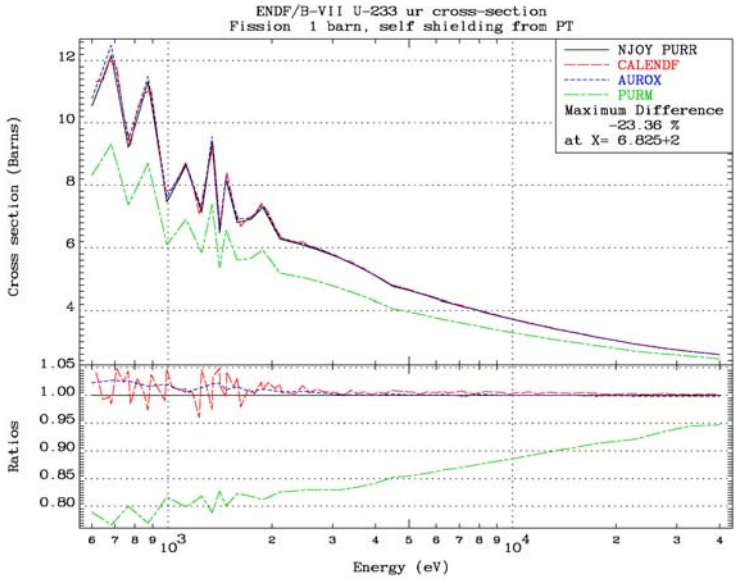
ENDF/B-VII U-233 ur cross-section
Fission 1 barn, self shielding from PT
Cross section (Barns)
NJOY PURR
CALENDF
AUROX
PURM
Maximum Difference
-23.36 %
at X= 6.825+2
Ratios
Energy (eV)

5.8 U-238 UR cross sections

This is the second of the two LSSF=1 evaluations, and, of course, a rather important one. The circa 1% differences between the CALENDF results and all the others are also due to the group structure differences that appear in the resolved range at the lowest energy and the continuum at the highest. It is interesting to note that this occurs only for the total and elastic channels. As a point of reference, and if PURM results are set aside, NJOY-PURR, AUROX and CALENDF agree within a 1% in computing the total, elastic and capture 1 barn effective cross sections of U-238. One may notice that here again, only CALENDF includes the inelastic channel from its probability tables and self-shield it as well with the competitive widths found in the file 2. This is unique behavior amongst these codes and perfectly legitimate (but often overlooked) by the ENDF-102 data format.

Figure 16 U-238 UR cross section comparison – 4 codes

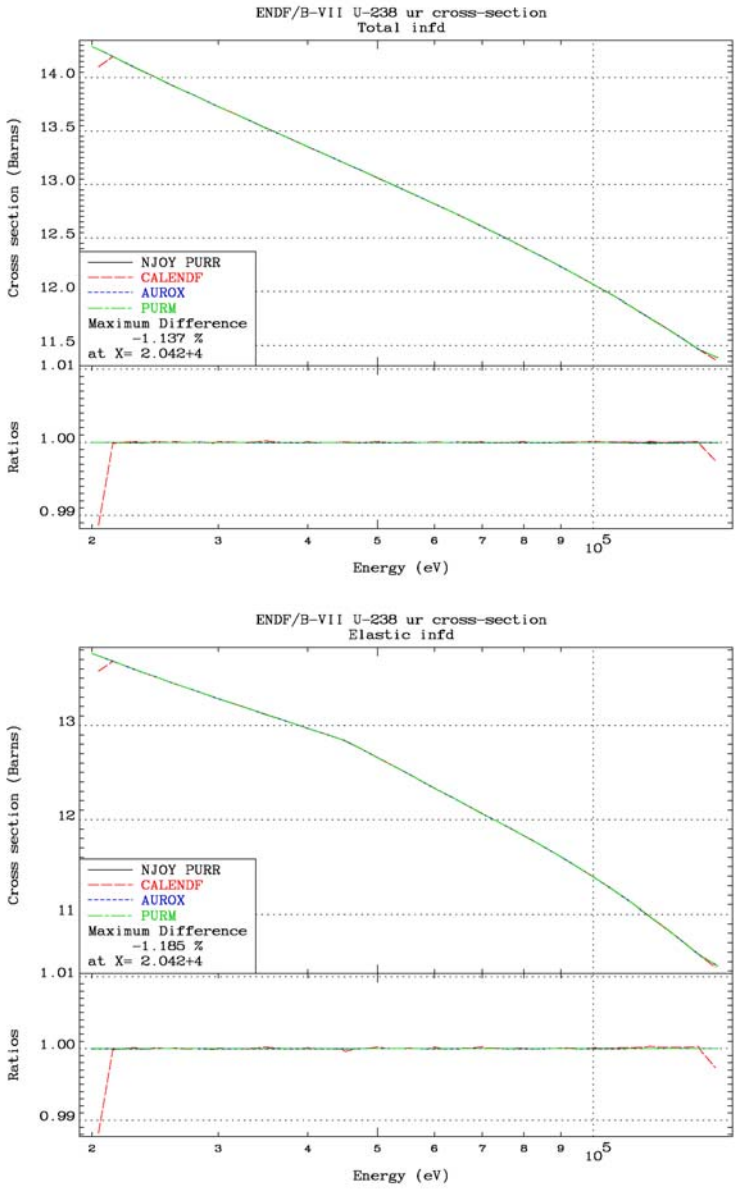

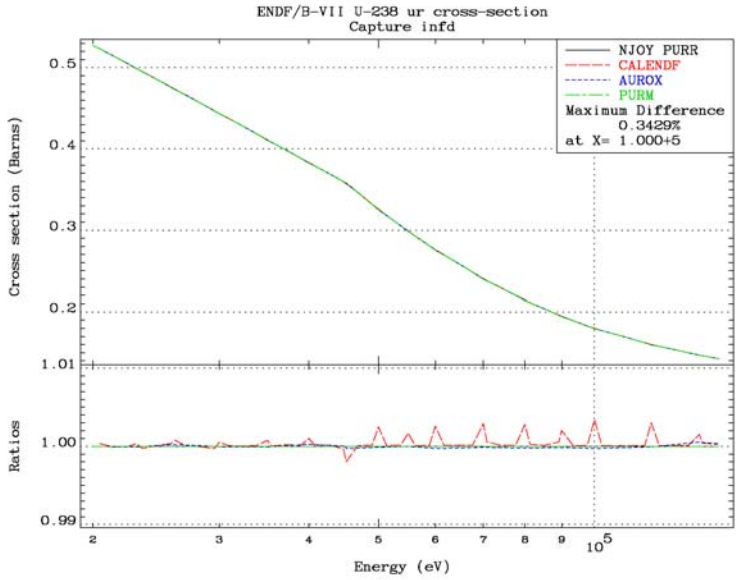
ENDF/B-VII U-238 ur cross-section
Capture infd
NJOY PURR
CALENDF
AUROX
PURM
Maximum Difference
0.3429%
at X= 1.000+5
Cross section (Barns)
Ratios
Energy (eV)

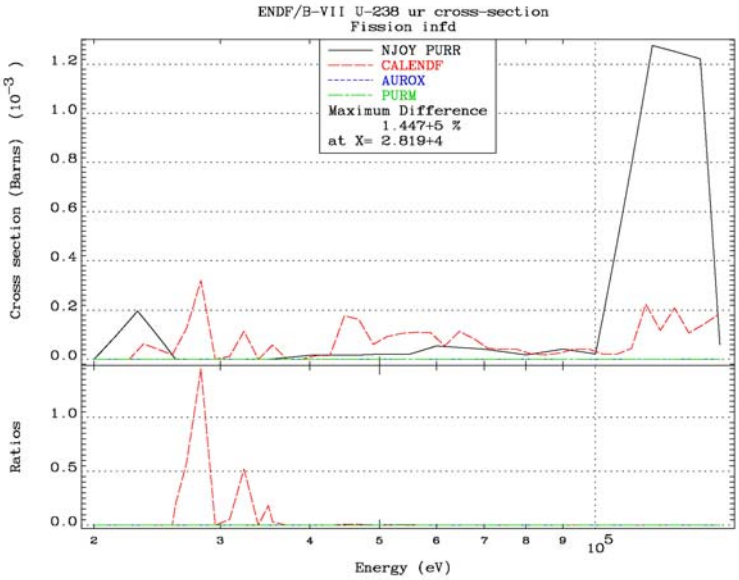
ENDF/B-VII U-238 ur cross-section
Fission infd
NJOY PURR
CALENDF
AUROX
PURM
Maximum Difference
1.447+5 %
at X= 2.819+4
Cross section (Barns) (10-3)
Ratios
Energy (eV)

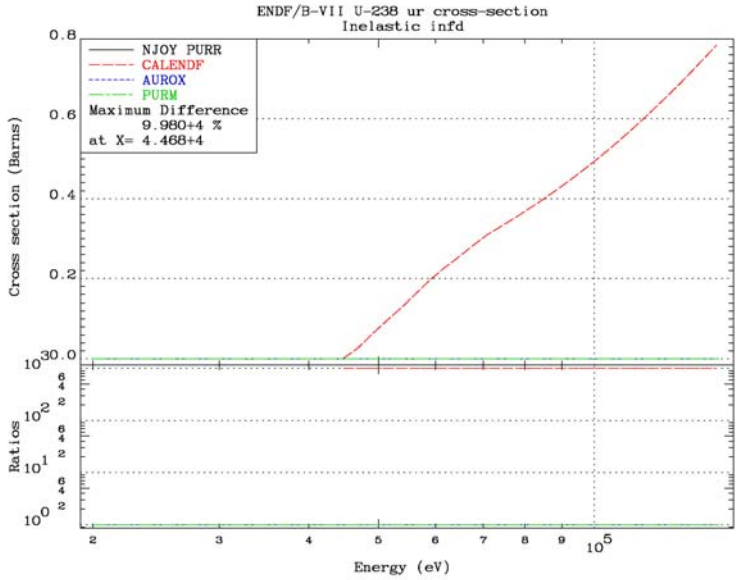
ENDF/B-VII U-238 ur cross-section
Inelastic infd
NJOY PURR
CALENDF
AUROX
PURM
Maximum Difference
9.980+4 %
at X= 4.468+4
Cross section (Barns)
Ratios
Energy (eV)

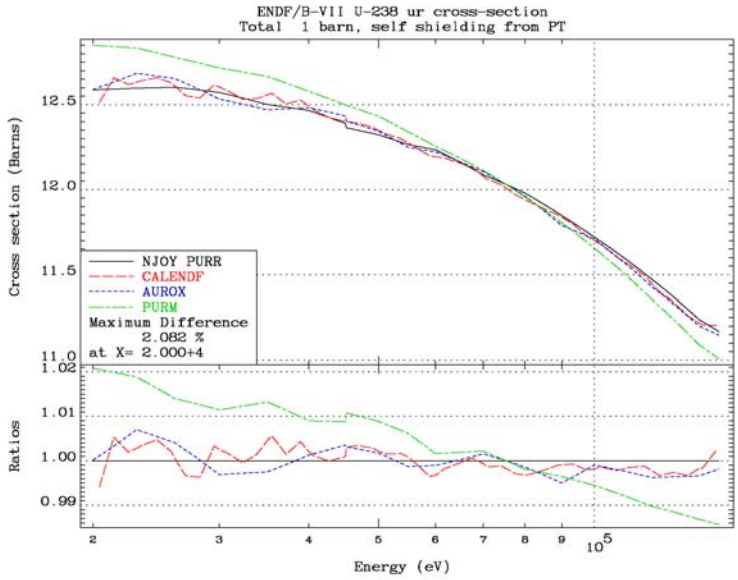
ENDF/B-VII U-238 ur cross-section
Total 1 barn, self shielding from PT
Cross section (Barns)
NJOY PURR
CALENDF
AUROX
PURM
Maximum Difference
2.082 %
at X= 2.000+4
Ratios
Energy (eV)

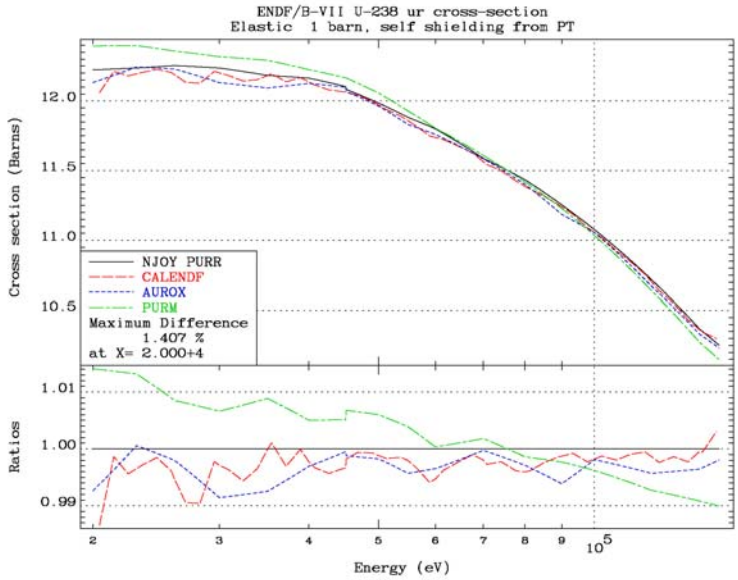
ENDF/B-VII U-238 ur cross-section
Elastic 1 barn, self shielding from PT
Cross section (Barns)
NJOY PURR
CALENDF
AUROX
PURM
Maximum Difference
1.407 %
at X= 2.000+4
Ratios
Energy (eV)

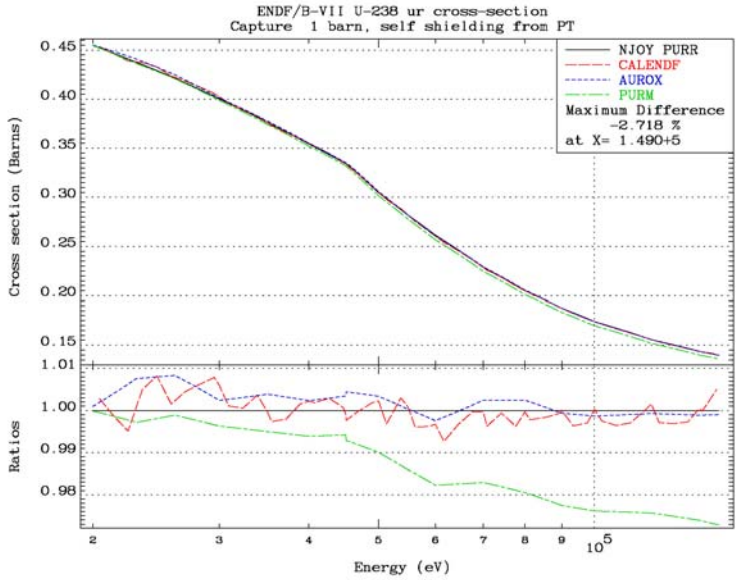
ENDF/B-VII U-238 ur cross-section
Capture 1 barn, self shielding from PT
Cross section (Barns)
NJOY PURR
CALENDF
AUROX
PURM
Maximum Difference
-2.718 %
at X= 1.490+5
Ratios
Energy (eV)

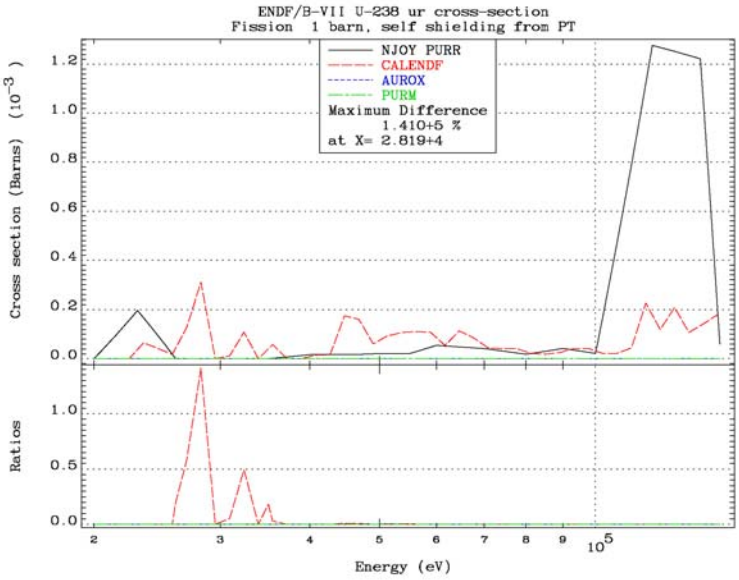
ENDF/B-VII U-238 ur cross-section
Fission 1 barn, self shielding from PT
NJOY PURR
CALENDF
AUROX
PURM
Maximum Difference
1.410+5 %
at X= 2.819+4
Cross section (Barns) (10^-3)
Ratios
Energy (eV)

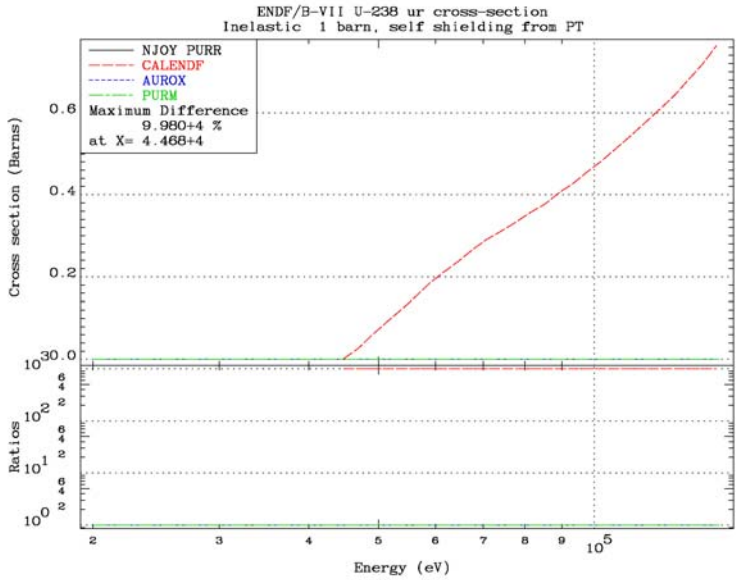
ENDF/B-VII U-238 ur cross-section
Inelastic 1 barn, self shielding from PT
NJOY PURR
CALENDF
AUROX
PURM
Maximum Difference
9.980+4 %
at X= 4.468+4
Cross section (Barns)
Ratios
Energy (eV)

5.9 W-184 UR cross sections

This is the only non-fissionable isotope compared in this work, and it is included to understand better our interpretation of a broad and shaped unresolved range. Here, CALENDF departs notably from the other codes in its cross section interpretation. It samples the parameters at deeper levels, and the results show more pronounced structure. Still, the four different codes' broad group averages show rather good agreement across this two-decade energy range. As before the humps demonstrate the impact of a cross section against parameters interpolations. It is notable in this case that the differences seen in the 1 barn self-shielded comparison do not show any clear pattern or trend, with differences rather uniform at around 20% levels.

Figure 17 W-184 UR cross section comparison – 4 codes

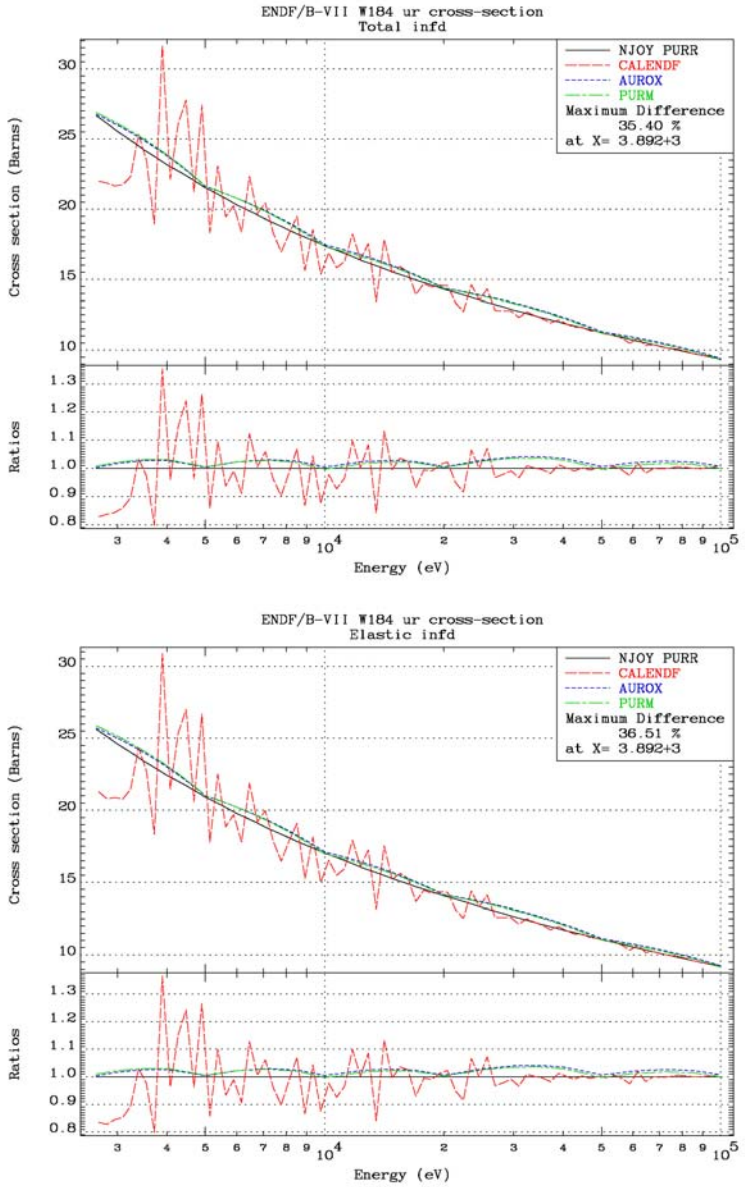

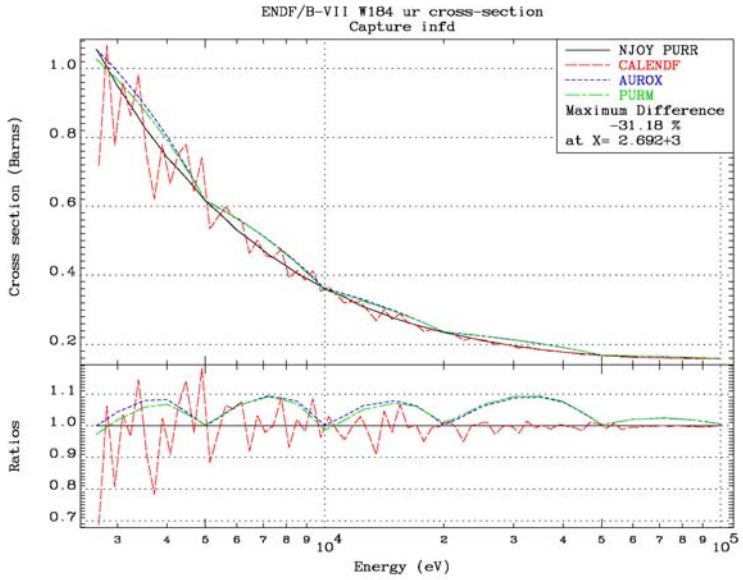
ENDF/B-VII W184 ur cross-section
Capture infd
NJOY PURR
CALENDF
AUROX
PURM
Maximum Difference
-31.18 %
at X= 2.692+3
Cross section (Barns)
Ratios
Energy (eV)

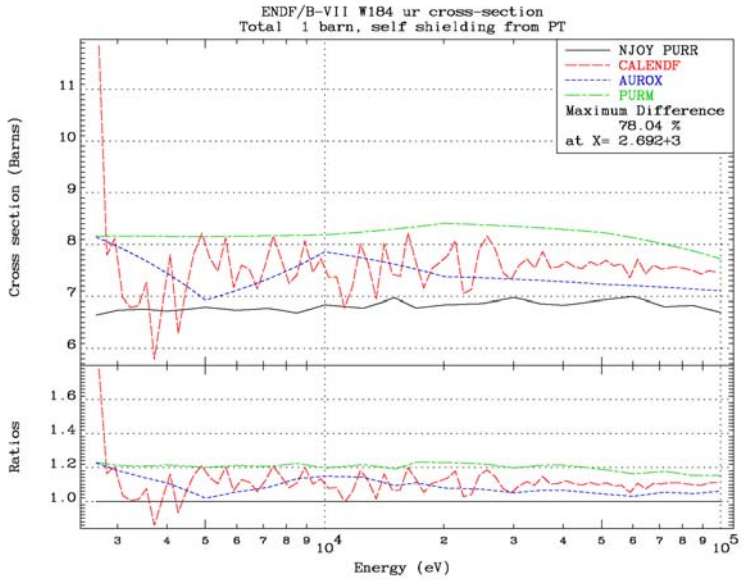
ENDF/B-VII W184 ur cross-section
Total 1 barn, self shielding from PT
NJOY PURR
CALENDF
AUROX
PURM
Maximum Difference
78.04 %
at X= 2.692+3
Cross section (Barns)
Ratios
Energy (eV)

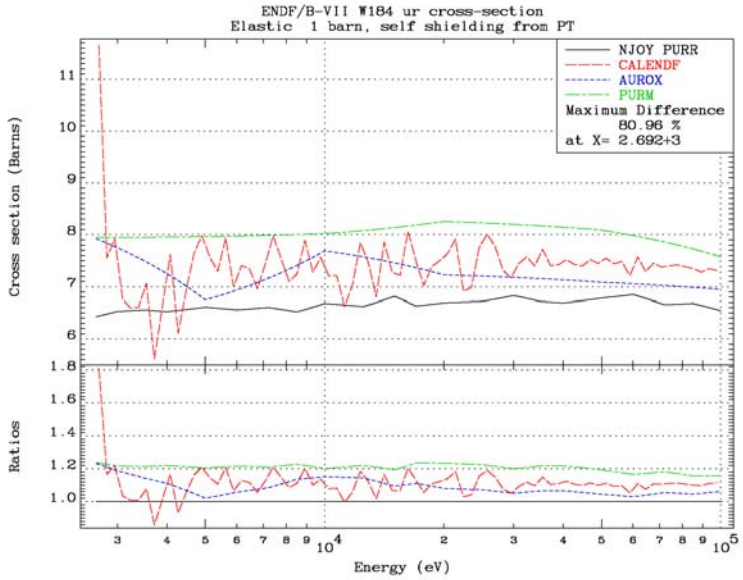
ENDF/B-VII W184 ur cross-section
Elastic 1 barn, self shielding from PT
NJOY PURR
CALENDF
AUROX
PURM
Maximum Difference
80.96 %
at X= 2.692+3
Cross section (Barns)
Ratios
Energy (eV)

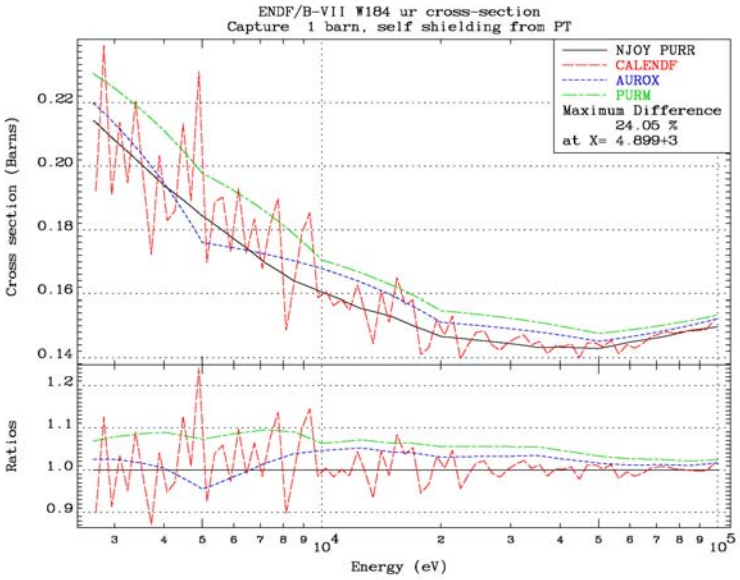

6 Conclusions

The primary conclusion is that these four processing codes usually agree within a target accuracy of 1% for both infinitely dilute and 1-barn self-shielded effective cross sections (with the exception of PURM) when the parameters files data and ENDF-102 rules have been properly and consistently interpreted by both the evaluators and those who processed the data. In our comparison, this only occurred on one fourth (1/4) of the evaluations, and when the LSSF=1 flag has been properly used. In all other cases, and due to a lack of clarity and constraints in the ENDF-102 data format, both infinitely dilute and self-shielded cross section results from those four codes can diverge significantly; well above the few percent frequently tolerated in this range for cross section averages and pointwise data. These variations in interpretation lead to some large differences between transport codes' results due to the cross sections. There seems to exist no one transport code that can make use of the output from more than one of theses processing codes (see Appendix B) and so singularly test their differences.

A secondary conclusion derives from the fact that processing codes have to palliate the data format deficiencies, either because the format rules have not been well defined, have been interpreted differently, or are inconsistent or unphysical. Typically, in the cases here, parameter interpolation gives better physical results than cross section interpolation based on file 2 interpolation specifications. Inconsistently applied unresolved resonance range parameters file will inevitably lead to different results.

Another secondary conclusion is that when the rule or data set are not properly pinned down, the processing codes will inevitably be developed to compensate. This is the case here when CALENDF, having read in the competition widths from U-238 file 2, is making use of them in self-shielding the inelastic competition. It is the only one of these processing codes doing so.

This study focuses on the data derived from probability table treatment in the unresolved resonance range, mostly but not uniquely used by Monte Carlo codes. Other self-shielding

methodologies that can be used in this range and below by other method may lead to even greater differences.

This study shows a clearer way forward on the issues of data formats, formalisms, and interpretation in the unresolved resonance range The ENDF-102 rules should be modified along the following lines:

- Privileges, enforces LSSF=1 formalism (self-shielding from file 2, cross section in file 3).
- Allow all competition channels to be open in this range, e.g., inelastic levels, direct components, charge particle emissions. This would make the sum-up and energy interpolation rules clear, but would not require that everybody could or should use them all.
- Account for the effect of multiple fission channels.
- Allow for other formalisms in the UR : MLBW, RML.
- Make the formats and specifications unambiguous.

One would like to remark at that deep level of interpretation that what is clearly written in a file is always better interpreted, although it may still be complemented and devise. What is not there, but is needed, will have to be generated and subject to interpretation.

References

[1] "A Code Comparison Study for the Bigten Critical Assembly", R. E. MacFarlane et al., Los Alamos National laboratory report, LA-UR-08-4668, July 2008. Available at http://t2.lanl.gov/publications/publications.html

[2] "**ENDF-102** ENDF-6 Data Formats and Procedures for the Evaluated Nuclear Data File ENDF-VII", M. Herman, ed., Brookhaven National Laboratory report BNL-NCS-44945-05-Rev., June 2005. Available at http://www.nndc.bnl.gov/publications/publications.html#manuals

[3] "**PREPRO 2007**: 2007 ENDF/B pre-processing Codes", Dermott E. Cullen, IAEA-NDS-39, Rev. 13, March 17, 2007, Nuclear Data Section, International Atomic Energy Agency, Vienna, Austria. Available at http://www-nds.iaea.or.at/ndspub/endf/prepro/

[4] "ENDF-102 unresolved range recommendations proposal", D. E. Cullen and R.E MacFarlane, February 2009. Available http://www.nndc.bnl.gov/csewg/formatprop.jsp

[5] "**The NJOY** Nuclear Data Processing System, Version 91," Los Alamos National Laboratory report LA-12740-M, by R. E. MacFarlane and D. W. Muir, (October 1994). For latest information, see http://t2.lanl.gov/codes/njoy99.

[6] "**U3R**, a Code to Calculate Unresolved Resonance Cross Section Probability Tables", AI-AEC-13024, by J. M. Otter, R. C. Lewis, and L. B. Levitt, July, 1972.

[7] "Calculating probability Tales for the Unresolved-Resonance Region Using Monte Carlo Methods", M.E. Dunn and L.C. Leal, Nuclear Science and Engineering: 148, 30-42 (2004).

[8] "**CALENDF-2005**: User manual", J-Ch. Sublet, P. Ribon and M. Coste-Delclaux, CEA-R-6131, ISSN 0429-3460, 2006. Available http://www.nea.fr/abs/html/nea-1278.html

[9] "**ENDF/B-VII.0**: Next Generation Evaluated Nuclear Data Library for Nuclear Science and Technology", M.B. Chadwick, P. Oblozinsky, M. Herman, N.M. Greene, R.D. McKnight, D.L.Smith, P.G. Young, R.E. MacFarlane, G.M. Hale, S.C. Frankle, A.C. Kahler, T. Kawano, R.C. Little, D.G. Madland, P. Moller, R.D. Mosteller, P.R. Page, P. Talou, H. Trellue, M.C. White, W.B. Wilson, R. Arcilla, C.L. Dunford, S.F. Mughabghab, B. Pritychenko, D. Rochman, A.A. Sonzogni, C.R. Lubitz, T.H. Trumbull, J.P. Weinman, D.A. Brown, D.E. Cullen, D.P. Heinrichs, D.P. McNabb, H. Derrien, M.E. Dunn, N.M. Larson, L.C. Leal, A.D. Carlson, R.C. Block, J.B. Briggs, E.T. Cheng, H.C. Huria, M.L. Zerkle, K.S. Kozier, A. Courcelle, V.Pronyaev and S.C. van der Marck, Nuclear Data Sheets, vol. 107, pp. 2931-3060, 2006.

[10] "Methods for Calculating Cross-sections and Shielding Factors in the Unresolved Resonance region", JEF/DOC-79, 1985. Available: http://www.nea.fr/html/dbdata/projects/jeffdoc.html

[11] "**TRIPOLI 4 User guide**", O. Petit, F-X. Hugot, Y-K. Lee, C. Jouanne, A. Mazzolo, CEA-R-6169, ISSN 0429-3460, 2008. Available at http://www.nea.fr/abs/html/nea-1716.html.

Appendix A

Here are the boundaries of the Red-616 group structure used by CALENDF.

```
2.00000E+07  1.99526E+07  1.90546E+07  1.81970E+07
1.73780E+07  1.65959E+07  1.58489E+07  1.51356E+07
1.44544E+07  1.38038E+07  1.31826E+07  1.25893E+07
1.20226E+07  1.14815E+07  1.09648E+07  1.04713E+07
1.00000E+07  9.54993E+06  9.12011E+06  8.70964E+06
8.31764E+06  7.94328E+06  7.58578E+06  7.24436E+06
6.91831E+06  6.60693E+06  6.30957E+06  6.02560E+06
5.75440E+06  5.49541E+06  5.24807E+06  5.01187E+06
4.78630E+06  4.57088E+06  4.36516E+06  4.16869E+06
3.98107E+06  3.80189E+06  3.63078E+06  3.46737E+06
3.31131E+06  3.16228E+06  3.01995E+06  2.88403E+06
2.75423E+06  2.63027E+06  2.51189E+06  2.39883E+06
2.29087E+06  2.18776E+06  2.08930E+06  1.99526E+06
1.90546E+06  1.81970E+06  1.73780E+06  1.65959E+06
1.58489E+06  1.51356E+06  1.44544E+06  1.38038E+06
1.31826E+06  1.25893E+06  1.20226E+06  1.14815E+06
1.09648E+06  1.04713E+06  1.00000E+06  9.54993E+05
9.12011E+05  8.70964E+05  8.31764E+05  7.94328E+05
7.58578E+05  7.24436E+05  6.91831E+05  6.60693E+05
6.30957E+05  6.02560E+05  5.75440E+05  5.49541E+05
5.24807E+05  5.01187E+05  4.78630E+05  4.57088E+05
4.36516E+05  4.16869E+05  3.98107E+05  3.80189E+05
3.63078E+05  3.46737E+05  3.31131E+05  3.16228E+05
3.01995E+05  2.88403E+05  2.75423E+05  2.63027E+05
2.51189E+05  2.39883E+05  2.29087E+05  2.18776E+05
2.08930E+05  1.99526E+05  1.90546E+05  1.81970E+05
1.73780E+05  1.65959E+05  1.58489E+05  1.51356E+05
1.44544E+05  1.38038E+05  1.31826E+05  1.25893E+05
1.20226E+05  1.14815E+05  1.09648E+05  1.04713E+05
1.00000E+05  9.54993E+04  9.12011E+04  8.70964E+04
8.31764E+04  7.94328E+04  7.58578E+04  7.24436E+04
6.91831E+04  6.60693E+04  6.30957E+04  6.02560E+04
5.75440E+04  5.49541E+04  5.24807E+04  5.01187E+04
4.78630E+04  4.57088E+04  4.36516E+04  4.16869E+04
3.98107E+04  3.80189E+04  3.63078E+04  3.46737E+04
3.31131E+04  3.16228E+04  3.01995E+04  2.88403E+04
2.75423E+04  2.63027E+04  2.51189E+04  2.39883E+04
2.29087E+04  2.18776E+04  2.08930E+04  1.99526E+04
1.90546E+04  1.81970E+04  1.73780E+04  1.65959E+04
1.58489E+04  1.51356E+04  1.44544E+04  1.38038E+04
1.31826E+04  1.25893E+04  1.20226E+04  1.14815E+04
1.09648E+04  1.04713E+04  1.00000E+04  9.54993E+03
9.12011E+03  8.70964E+03  8.31764E+03  7.94328E+03
7.58578E+03  7.24436E+03  6.91831E+03  6.60693E+03
6.30957E+03  6.02560E+03  5.75440E+03  5.49541E+03
5.24807E+03  5.01187E+03  4.78630E+03  4.57088E+03
4.36516E+03  4.16869E+03  3.98107E+03  3.80189E+03
3.63078E+03  3.46737E+03  3.31131E+03  3.16228E+03
3.01995E+03  2.88403E+03  2.75423E+03  2.63027E+03
2.51189E+03  2.39883E+03  2.29087E+03  2.18776E+03
2.08930E+03  1.99526E+03  1.90546E+03  1.81970E+03
1.73780E+03  1.65959E+03  1.58489E+03  1.51356E+03
1.44544E+03  1.38038E+03  1.31826E+03  1.25893E+03
1.20226E+03  1.14815E+03  1.09648E+03  1.04713E+03
1.00000E+03  9.54993E+02  9.12011E+02  8.70964E+02
8.31764E+02  7.94328E+02  7.58578E+02  7.24436E+02
6.91831E+02  6.60693E+02  6.30957E+02  6.02560E+02
5.75440E+02  5.49541E+02  5.24807E+02  5.01187E+02
4.78630E+02  4.57088E+02  4.36516E+02  4.16869E+02
3.98107E+02  3.80189E+02  3.63078E+02  3.46737E+02
3.31131E+02  3.16228E+02  3.01995E+02  2.88403E+02
2.75423E+02  2.63027E+02  2.51189E+02  2.39883E+02
2.29087E+02  2.18776E+02  2.08930E+02  1.99526E+02
```

1.90546E+02 1.81970E+02 1.73780E+02 1.65959E+02
1.58489E+02 1.51356E+02 1.44544E+02 1.38038E+02
1.31826E+02 1.25893E+02 1.20226E+02 1.14815E+02
1.09648E+02 1.04713E+02 1.00000E+02 9.54993E+01
9.12011E+01 8.70964E+01 8.31764E+01 7.94328E+01
7.58578E+01 7.24436E+01 6.91831E+01 6.60693E+01
6.30957E+01 6.02560E+01 5.75440E+01 5.49541E+01
5.24807E+01 5.01187E+01 4.78630E+01 4.57088E+01
4.36516E+01 4.16869E+01 3.98107E+01 3.80189E+01
3.63078E+01 3.46737E+01 3.31131E+01 3.16228E+01
3.01995E+01 2.88403E+01 2.75423E+01 2.63027E+01
2.51189E+01 2.39883E+01 2.29087E+01 2.18776E+01
2.08930E+01 1.99526E+01 1.90546E+01 1.81970E+01
1.73780E+01 1.65959E+01 1.58489E+01 1.51356E+01
1.44544E+01 1.38038E+01 1.31826E+01 1.25893E+01
1.20226E+01 1.14815E+01 1.09648E+01 1.04713E+01
1.00000E+01 9.54993E+00 9.12011E+00 8.70964E+00
8.31764E+00 7.94328E+00 7.58578E+00 7.24436E+00
6.91831E+00 6.60693E+00 6.30957E+00 6.02560E+00
5.75440E+00 5.49541E+00 5.24807E+00 5.01187E+00
4.78630E+00 4.57088E+00 4.36516E+00 4.16869E+00
3.98107E+00 3.80189E+00 3.63078E+00 3.46737E+00
3.31131E+00 3.16228E+00 3.01995E+00 2.88403E+00
2.75423E+00 2.63027E+00 2.51189E+00 2.39883E+00
2.29087E+00 2.18776E+00 2.08930E+00 1.99526E+00
1.90546E+00 1.81970E+00 1.73780E+00 1.65959E+00
1.58489E+00 1.51356E+00 1.44544E+00 1.38038E+00
1.31826E+00 1.25893E+00 1.20226E+00 1.14815E+00
1.09648E+00 1.04713E+00 1.00000E+00 9.54993E-01
9.12011E-01 8.70964E-01 8.31764E-01 7.94328E-01
7.58578E-01 7.24436E-01 6.91831E-01 6.60693E-01
6.30957E-01 6.02560E-01 5.75440E-01 5.49541E-01
5.24807E-01 5.01187E-01 4.78630E-01 4.57088E-01
4.36516E-01 4.16869E-01 3.98107E-01 3.80189E-01
3.63078E-01 3.46737E-01 3.31131E-01 3.16228E-01
3.01995E-01 2.88403E-01 2.75423E-01 2.63027E-01
2.51189E-01 2.39883E-01 2.29087E-01 2.18776E-01
2.08930E-01 1.99526E-01 1.90546E-01 1.81970E-01
1.73780E-01 1.65959E-01 1.58489E-01 1.51356E-01
1.44544E-01 1.38038E-01 1.31826E-01 1.25893E-01
1.20226E-01 1.14815E-01 1.09648E-01 1.04713E-01
1.00000E-01 9.54993E-02 9.12011E-02 8.70964E-02
8.31764E-02 7.94328E-02 7.58578E-02 7.24436E-02
6.91831E-02 6.60693E-02 6.30957E-02 6.02560E-02
5.75440E-02 5.49541E-02 5.24807E-02 5.01187E-02
4.78630E-02 4.57088E-02 4.36516E-02 4.16869E-02
3.98107E-02 3.80189E-02 3.63078E-02 3.46737E-02
3.31131E-02 3.16228E-02 3.01995E-02 2.88403E-02
2.75423E-02 2.63027E-02 2.51189E-02 2.39883E-02
2.29087E-02 2.18776E-02 2.08930E-02 1.99526E-02
1.90546E-02 1.81970E-02 1.73780E-02 1.65959E-02
1.58489E-02 1.51356E-02 1.44544E-02 1.38038E-02
1.31826E-02 1.25893E-02 1.20226E-02 1.14815E-02
1.09648E-02 1.04713E-02 1.00000E-02 9.54993E-03
9.12011E-03 8.70964E-03 8.31764E-03 7.94328E-03
7.58578E-03 7.24436E-03 6.91831E-03 6.60693E-03
6.30957E-03 6.02560E-03 5.75440E-03 5.49541E-03
5.24807E-03 5.01187E-03 4.78630E-03 4.57088E-03
4.36516E-03 4.16869E-03 3.98107E-03 3.80189E-03
3.63078E-03 3.46737E-03 3.31131E-03 3.16228E-03
3.01995E-03 2.88403E-03 2.75423E-03 2.63027E-03
2.51189E-03 2.39883E-03 2.29087E-03 2.18776E-03
2.08930E-03 1.99526E-03 1.90546E-03 1.81970E-03
1.73780E-03 1.65959E-03 1.58489E-03 1.51356E-03
1.44544E-03 1.38038E-03 1.31826E-03 1.25893E-03
1.20226E-03 1.14815E-03 1.09648E-03 1.04713E-03
1.00000E-03 9.54993E-04 9.12011E-04 8.70964E-04
8.31764E-04 7.94328E-04 7.58578E-04 7.24436E-04
6.91831E-04 6.60693E-04 6.30957E-04 6.02560E-04
5.75440E-04 5.49541E-04 5.24807E-04 5.01187E-04
4.78630E-04 4.57088E-04 4.36516E-04 4.16869E-04
3.98107E-04 3.80189E-04 3.63078E-04 3.46737E-04

```
3.31131E-04  3.16228E-04  3.01995E-04  2.88403E-04
2.75423E-04  2.63027E-04  2.51189E-04  2.39883E-04
2.29087E-04  2.18776E-04  2.08930E-04  1.99526E-04
1.90546E-04  1.81970E-04  1.73780E-04  1.65959E-04
1.58489E-04  1.51356E-04  1.44544E-04  1.38038E-04
1.31826E-04  1.25893E-04  1.20226E-04  1.14815E-04
1.09648E-04  1.04713E-04  1.00000E-04  9.54993E-05
9.12011E-05  8.70964E-05  8.31764E-05  7.94328E-05
7.58578E-05  7.24436E-05  6.91831E-05  6.60693E-05
6.30957E-05  6.02560E-05  5.75440E-05  5.49541E-05
5.24807E-05  5.01187E-05  4.78630E-05  4.57088E-05
4.36516E-05  4.16869E-05  3.98107E-05  3.80189E-05
3.63078E-05  3.46737E-05  3.31131E-05  3.16228E-05
3.01995E-05  2.88403E-05  2.75423E-05  2.63027E-05
2.51189E-05  2.39883E-05  2.29087E-05  2.18776E-05
2.08930E-05  1.99526E-05  1.90546E-05  1.81970E-05
1.73780E-05  1.65959E-05  1.58489E-05  1.51356E-05
1.44544E-05  1.38038E-05  1.31826E-05  1.25893E-05
1.20226E-05  1.14815E-05  1.09648E-05  1.04713E-05
1.00000E-05
```

Appendix B

CALENDF - Pu239 2950 eV probability table
NOR = 8, table order
NPAR = 3, partials; elastic, absorption, fission
I = -7, first negative moments

```
tables de probabilite pour  94-Pu-239 LANL       DIST-DEC06
 ZA= 94239. MAT=9437 TEFF= 293.6   54 groupes de 2.5119E+3 a 3.0200E+4 IPRECI=4
IG  193 ENG=2.884030E+3 3.019950E+3 NOR= 8 I= -7 NPAR=3 KP=   2 101  18   0   0
  1.445989-2  9.275984+0  7.938243+0  3.784994-1  9.592410-1
  2.530904-1  1.204427+1  1.050705+1  4.120089-1  1.125216+0
  3.786562-1  1.597588+1  1.196700+1  1.341964+0  2.666910+0
  2.264860-1  2.397558+1  1.420897+1  3.557534+0  6.209075+0
  9.747106-2  3.855881+1  2.245308+1  7.251606+0  8.854119+0
  2.563850-2  6.079895+1  3.779216+1  1.117563+1  1.183115+1
  3.701015-3  9.447885+1  6.799134+1  1.523110+1  1.125642+1
  4.970289-4  1.325152+2  1.094414+2  1.423427+1  8.839522+0
 Probability    Total       Elastic   Absorption    Fission
```

CALENDF - SIGTTEUM - Pu239 2950 eV average value

```
  2.370043+1   1.663062+1   3.709518+0   3.360296+0
  Total        Elastic      Capture      Fission
```

PURM - Pu239 2950 eV probability table

FINAL TABLE

Table 6, Energy Point for Table: 2.95000E+03 eV
SigAve: 2.35776E+01 1.64716E+01 3.39770E+00 3.70829E+00 0.00000E+00 (tcfso)

Band	Band limits	Cummulative	Probability	Total	Capture	Fission	Scatter	Other
1	1.0758E+01	1.2943E-01	1.2943E-01	1.1458E+01	2.5003E-01	3.9960E-01	1.0808E+01	0.0000E+00
2	1.1966E+01	2.8050E-01	1.5107E-01	1.2593E+01	6.2297E-01	8.8073E-01	1.1089E+01	0.0000E+00
3	1.3311E+01	3.8999E-01	1.0949E-01	1.4011E+01	1.2240E+00	1.4405E+00	1.1347E+01	0.0000E+00
4	1.4806E+01	4.7698E-01	8.6989E-02	1.5592E+01	1.8691E+00	1.9774E+00	1.1746E+01	0.0000E+00
5	1.6468E+01	5.5164E-01	7.4667E-02	1.7357E+01	2.5440E+00	2.5174E+00	1.2296E+01	0.0000E+00
6	1.8318E+01	6.1630E-01	6.4656E-02	1.9300E+01	3.2150E+00	3.1232E+00	1.2962E+01	0.0000E+00
7	2.0376E+01	6.7261E-01	5.6311E-02	2.1492E+01	3.9796E+00	3.6814E+00	1.3831E+01	0.0000E+00
8	2.2664E+01	7.2279E-01	5.0178E-02	2.3895E+01	4.5942E+00	4.4480E+00	1.4853E+01	0.0000E+00
9	2.5210E+01	7.6789E-01	4.5100E-02	2.6558E+01	5.3440E+00	5.0476E+00	1.6166E+01	0.0000E+00
10	2.8041E+01	8.0623E-01	3.8344E-02	2.9550E+01	6.1162E+00	5.7205E+00	1.7713E+01	0.0000E+00
11	3.1191E+01	8.4000E-01	3.3767E-02	3.2880E+01	6.9616E+00	6.2504E+00	1.9668E+01	0.0000E+00
12	3.4694E+01	8.6961E-01	2.9611E-02	3.6562E+01	7.6667E+00	6.9653E+00	2.1930E+01	0.0000E+00
13	3.8590E+01	8.9520E-01	2.5589E-02	4.0709E+01	8.5789E+00	7.5763E+00	2.4554E+01	0.0000E+00
14	4.2925E+01	9.1764E-01	2.2444E-02	4.5167E+01	9.2099E+00	8.5327E+00	2.7424E+01	0.0000E+00
15	4.7746E+01	9.3542E-01	1.7778E-02	5.0309E+01	9.8300E+00	9.4260E+00	3.1053E+01	0.0000E+00
16	5.3109E+01	9.5150E-01	1.6078E-02	5.5847E+01	1.1088E+01	9.5642E+00	3.5194E+01	0.0000E+00
17	5.9074E+01	9.6306E-01	1.1556E-02	6.2244E+01	1.1644E+01	1.0592E+01	4.0008E+01	0.0000E+00
18	6.5708E+01	9.7198E-01	8.9222E-03	6.9306E+01	1.2477E+01	1.0466E+01	4.6363E+01	0.0000E+00
19	7.3089E+01	9.8071E-01	8.7333E-03	7.7202E+01	1.4113E+01	8.5620E+00	5.4527E+01	0.0000E+00
20	8.1298E+01	1.0000E+00	1.9289E-02	1.0189E+02	1.7977E+01	1.0432E+01	7.3486E+01	0.0000E+00
	9.0429E+01							

AUROX - Pu239 2950 eV probability table

INDEX	CUM. PROB.	TOTAL XSEC	ELASTIC	FISSION
1	1.45525E-02	1.04826E+01	9.11199E+00	1.03418E+00
2	3.16110E-02	1.10850E+01	9.77098E+00	9.92191E-01
3	6.52933E-02	1.14058E+01	1.00173E+01	1.06561E+00
4	1.20041E-01	1.17532E+01	1.03083E+01	1.09848E+00
5	1.94416E-01	1.21018E+01	1.05319E+01	1.20375E+00
6	2.86526E-01	1.24702E+01	1.07881E+01	1.27943E+00
7	3.88354E-01	1.28405E+01	1.10111E+01	1.39126E+00
8	4.88874E-01	1.32258E+01	1.12556E+01	1.49212E+00
9	5.84038E-01	1.36305E+01	1.15180E+01	1.59540E+00
10	6.72148E-01	1.40430E+01	1.17578E+01	1.72737E+00
11	7.48130E-01	1.44630E+01	1.20270E+01	1.83605E+00
12	8.10114E-01	1.48995E+01	1.23176E+01	1.94907E+00
13	8.60227E-01	1.53499E+01	1.26796E+01	2.00309E+00
14	8.97912E-01	1.58165E+01	1.30367E+01	2.07655E+00
15	9.24842E-01	1.62938E+01	1.34119E+01	2.14404E+00
16	9.45576E-01	1.67868E+01	1.37613E+01	2.26831E+00
17	9.60244E-01	1.73025E+01	1.41483E+01	2.37176E+00
18	9.72256E-01	1.78255E+01	1.45391E+01	2.47680E+00
19	9.91565E-01	1.88066E+01	1.54151E+01	2.53128E+00
20	1.00000E+00	2.11962E+01	1.75584E+01	2.73069E+00
Average		1.37738E+01	1.16412E+01	1.61124E+00

NJOY-PURR - Pu239 2950 eV probability table

```
probability table
tmin 2.936E+02 5.027E+00
tmax 2.936E+02 6.131E+00 8.366E+00 9.660E+00 1.063E+01 1.139E+01 1.263E+01 1.373E+01 1.496E+01 1.630E+01 1.780E+01
               1.993E+01 2.258E+01 2.684E+01 3.409E+01 4.857E+01 6.522E+01 8.073E+01 8.827E+01 1.036E+02 1.513E+02
prob 2.936E+02 7.344E-05 2.705E-03 1.092E-02 2.261E-02 3.487E-02 8.695E-02 8.645E-02 8.649E-02 7.910E-02 7.232E-02
               8.273E-02 7.824E-02 9.087E-02 9.785E-02 9.521E-02 4.175E-02 1.713E-02 8.628E-03 3.866E-03 1.238E-03
tot  2.936E+02 5.791E+00 7.783E+00 9.170E+00 1.022E+01 1.104E+01 1.204E+01 1.318E+01 1.433E+01 1.561E+01 1.702E+01
               1.882E+01 2.118E+01 2.457E+01 3.016E+01 4.018E+01 5.534E+01 7.293E+01 8.398E+01 9.361E+01 1.148E+02
els  2.936E+02 4.289E+00 6.468E+00 7.875E+00 8.927E+00 9.701E+00 1.048E+01 1.117E+01 1.170E+01 1.217E+01 1.267E+01
               1.331E+01 1.427E+01 1.580E+01 1.880E+01 2.510E+01 3.620E+01 5.183E+01 6.189E+01 6.578E+01 7.881E+01
fis  2.936E+02 9.861E-01 8.062E-01 7.641E-01 7.706E-01 8.074E-01 9.272E-01 1.134E+00 1.422E+00 1.790E+00 2.197E+00
               2.704E+00 3.331E+00 4.175E+00 5.293E+00 6.938E+00 8.719E+00 8.901E+00 7.593E+00 1.143E+01 1.665E+01
cap  2.936E+02 5.166E-01 5.086E-01 5.308E-01 5.179E-01 5.291E-01 6.350E-01 8.694E-01 1.209E+00 1.646E+00 2.152E+00
               2.804E+00 3.579E+00 4.595E+00 6.071E+00 8.137E+00 1.043E+01 1.220E+01 1.450E+01 1.640E+01 1.933E+01
```

ÉDITÉ PAR
LA DIRECTION DES SYSTEMES
D'INFORMATION

CEA / SACLAY 91191 GIF-SUR-YVETTE CEDEX FRANCE